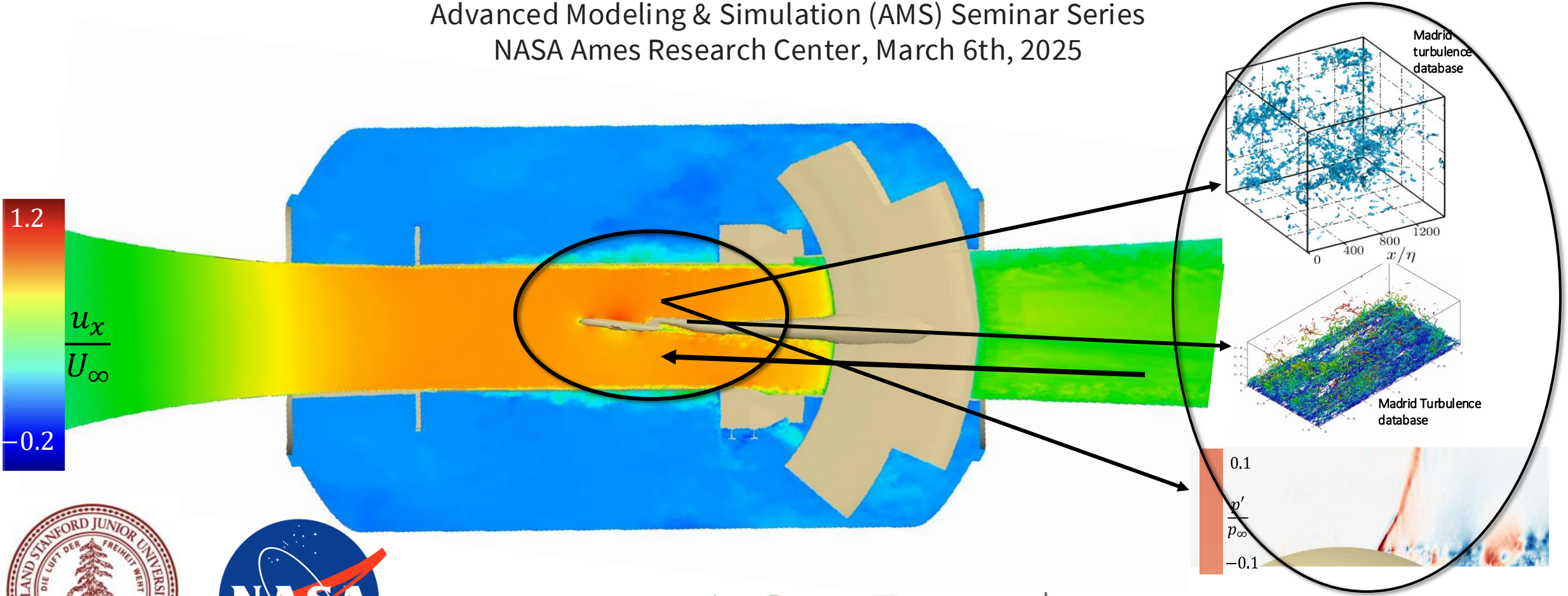
Modeling, simulations, and analysis of turbulent boundary layers exhibiting smooth-body separation

Rahul Agrawal

Advanced Modeling & Simulation (AMS) Seminar Series
NASA Ames Research Center, March 6th, 2025

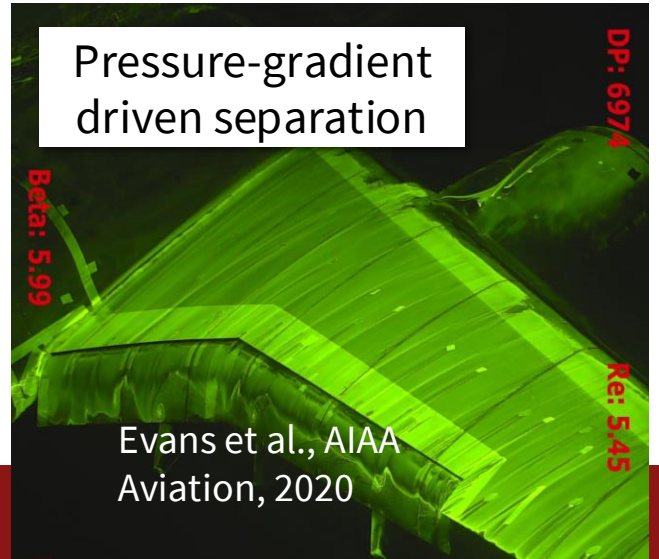


Leland Stanford Junior University
NASA
BOEING
OAK RIDGE National Laboratory | LEADERSHIP COMPUTING FACILITY
CTR Stanford University CENTER FOR TURBULENCE RESEARCH

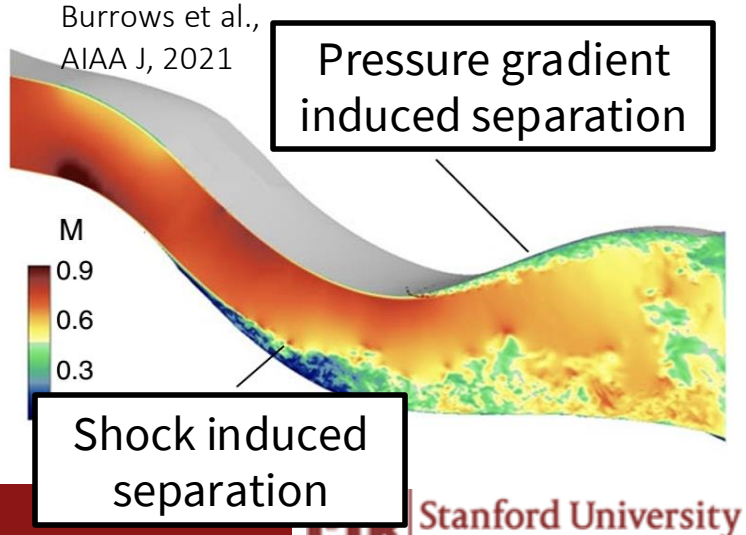
Pressure-gradient boundary layers in engineering

- In practical engineering flows, boundary layers are often **skewed,** undergo **turbulent separation** due to **pressure-gradients, curvature, shock** effects
  - **Smooth body separation**: Sepn. point is not geometrically imposed; dependent on external forces.

- **Reynolds number of such flows is large for high-fidelity, direct-numerical simulations (DNS)**
  - Cheaper simulation techniques:
    - **Reynolds averaged mean flow (RANS)**: solve for the mean flow, model entire turbulence
    - **Large-eddy simulations (LES)**: resolve large-scale flow, model smaller-scale motion



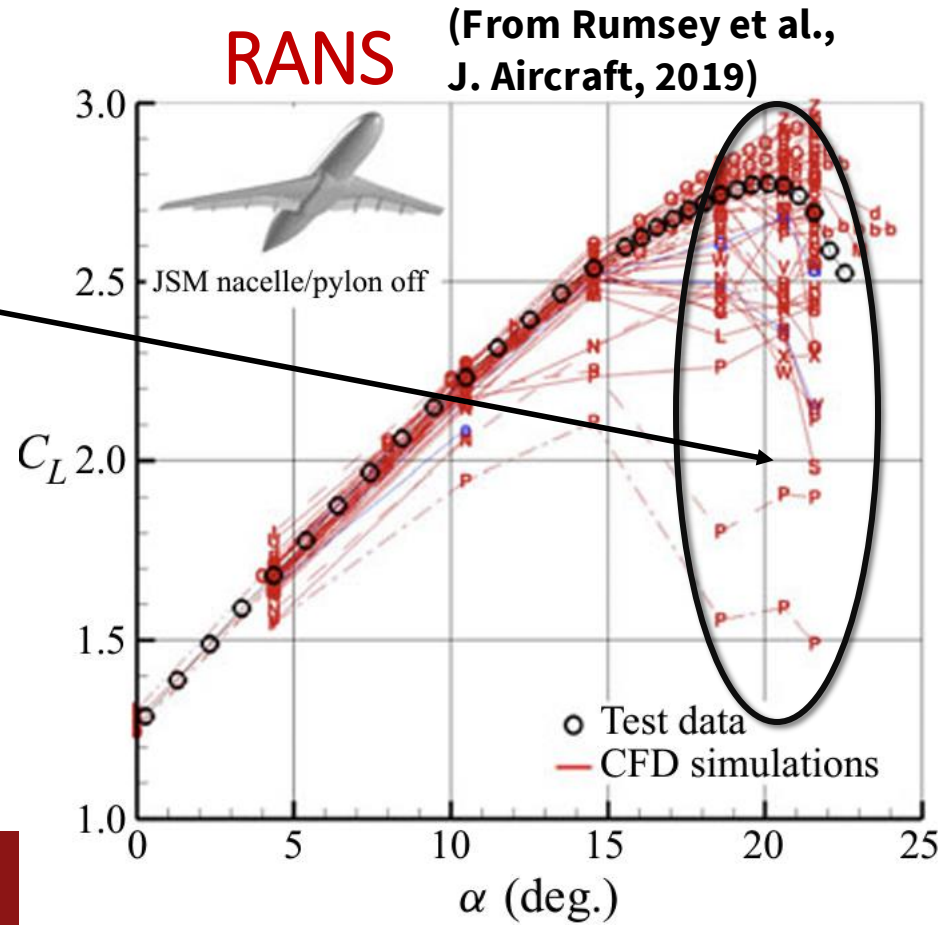




Need of LES in engineering flows

- Growing evidence: conventional RANS produces large spreads and inaccuracies in engineering flows
  - **Large unsteadiness, three-dimensional separations**

- **In high-lift aircraft systems, RANS produces large solution variability across models, codes**
  - **Spreads as large as $\Delta C_L \geq 0.50$ observed**
  - **Industry tolerance, $\Delta C_L = \pm 0.03$**
    (Clark, AIAA Aviation 2020)
  - Recent AIAA workshops have suggested smaller solution variability across LES methods
    (Kiris et al., HLPW5, 2024)



Governing equations for large-eddy simulations

- Filter governing equations (Navier-Stokes) to obtain evolution equations of **coarse-grained** velocity, pressure, density and temperature fields

$\tilde{f} = \overline{\rho f}/\bar{\rho}$ where $\bar{\cdot}$ denotes Reynolds filtering

$$\frac{\partial \bar{\rho}}{\partial t} + \frac{\partial \bar{\rho}\tilde{u}_j}{\partial x_j} = 0$$

$$\frac{\partial \bar{\rho}\tilde{u}_i}{\partial t} + \frac{\partial \bar{\rho}\tilde{u}_i\tilde{u}_j}{\partial x_j} + \frac{\partial \bar{p}}{\partial x_i} = \frac{\partial \sigma_{ij}(\bar{\rho}, \tilde{u}_i)}{\partial x_j} - \frac{\partial \boldsymbol{\tau_{ij}^{SGS}}}{\partial x_j}$$

Subgrid-scale stress: needs modeling

$$\frac{\partial \bar{E}}{\partial t} + \frac{\partial\left[(\bar{E} + \bar{p})\tilde{u}_j\right]}{\partial x_j} = \frac{\partial}{\partial x_j}\left(\frac{k\partial \bar{T}}{\partial x_j}\right) + \frac{\partial\left(\tilde{u}_i\sigma_{ij}(\bar{\rho}, \tilde{u}_i)\right)}{\partial x_j} - \frac{\partial \boldsymbol{Q_j^{SGS}}}{\partial x_j} - \frac{\partial\left(\tilde{u}_i\tau_{ij}^{SGS}\right)}{\partial x_j}$$

Subgrid heat flux: needs modeling

`

Conventional subgrid-scale model: dynamic Smagorinsky model (DSM)

- **Model form** (for incompressible eqns.):

Boussinesq Approximation $\longrightarrow$ $\tau_{ij}^{sgs} - \frac{1}{3}\delta_{ij}\tau_{kk}^{sgs} = -2\,C_s|\bar{S}|\Delta^2\,\bar{S}_{ij}$

Assumes the alignment b/w τ_{ij}, S_{ij}

Clark, Ferziger and Reynolds, JFM 1979; Meneveau & Katz, ARFM, 2000 showed $\mathbf{corr}\left(\tau_{ij}^{sgs},\ \bar{S}_{ij}\right) \sim \mathbf{10-20\%}$

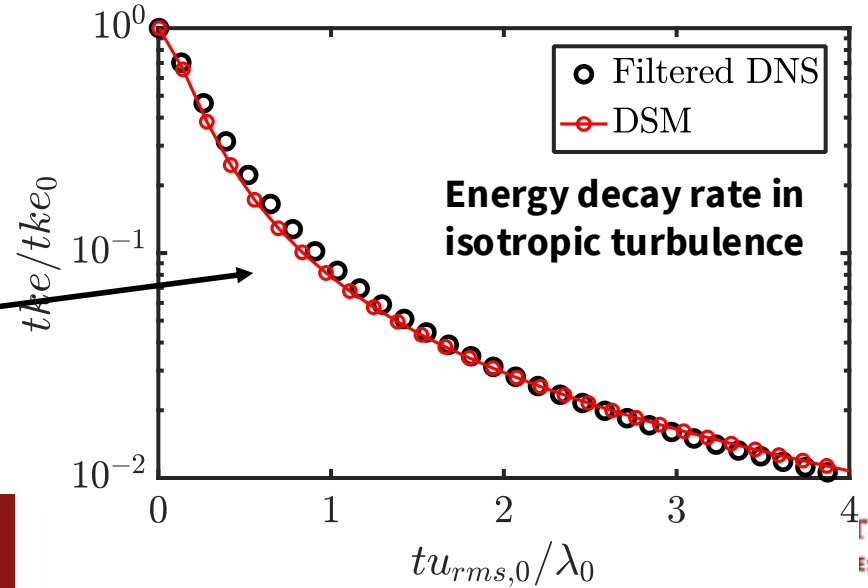
- **Germano et al., 1991 and Moin et al., 1991** developed a "dynamic procedure" for determining the subgrid model coefficient on the fly.

$$L_{ij} - \frac{1}{3}\,L_{kk} = -2\,(C_s\Delta^2)\,M_{ij}$$

Dynamic Smagorinsky model (DSM)

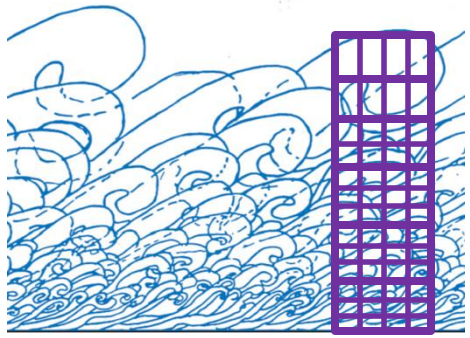
$$L_{ij} = \widehat{\bar{u}_i\bar{u}_j} - \hat{\bar{u}}_i\hat{\bar{u}}_j \text{ and } M_{ij} = \left(\frac{\hat{\Delta}}{\Delta}\right)^2 \widehat{|\bar{S}|\bar{S}_{ij}} - \widehat{|\bar{S}|\bar{S}_{ij}}$$

- Using least-squares procedure allows computing $(C_s\Delta^2)$
  - **Validated a-posteriori in canonical isotropic and wall-bounded flows[1]**

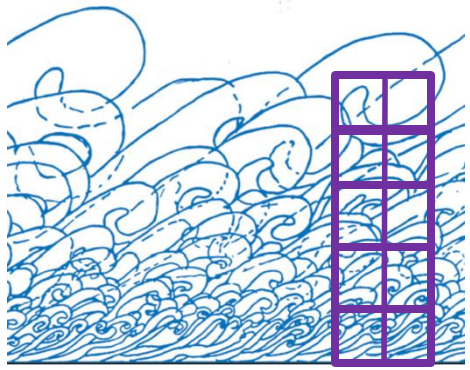


Different LES methodologies for wall-bounded flows

- **Wall-resolved LES:** resolve near wall energetic structures, coarser grids far from wall
  - Energetic eddies near wall are much smaller than geometric scales
  - **No slip BCs**
  - Grid-scaling: $N_{cv} \sim Re^{1.86}$ **(Choi and Moin, 2012; Yang and Griffin, 2021)**



- **Wall-modeled LES:** inner flow is subgrid, approximate boundary conditions (BCs) applied to provide correct wall stress
  - Grid-scaling: $N_{cv} \sim Re^{1}$ **(Choi and Moin, 2012; Yang and Griffin, 2021)**
  - Since BCs are approximate, the cost scaling is a function of their accuracy



Marusic and Monty, ARFM, 2019

Conventional (equilibrium) wall closure in wall-modeled LES

- **Wall model:** reduced order model for determining wall-quantities
- **Equilibrium wall model[1]:** RANS assumptions for mean velocity

$$\frac{dU^{RANS}}{dy} = \frac{\tau_w}{\nu + \nu_t^{RANS}}$$

$$\frac{\nu_t^{RANS}}{\nu} = \kappa y^+ \left(1 - exp\left(-\frac{y^+}{17}\right)\right)^2$$

Wall-stress

$$u_\tau = \sqrt{\tau_w/\rho}, U^+ = U/u_\tau, \quad y^+ = yu_\tau/\nu$$

Iterative solve for u_τ until the integration of the ODE leads to U^{RANS} matches the LES velocity u_i at the matching height

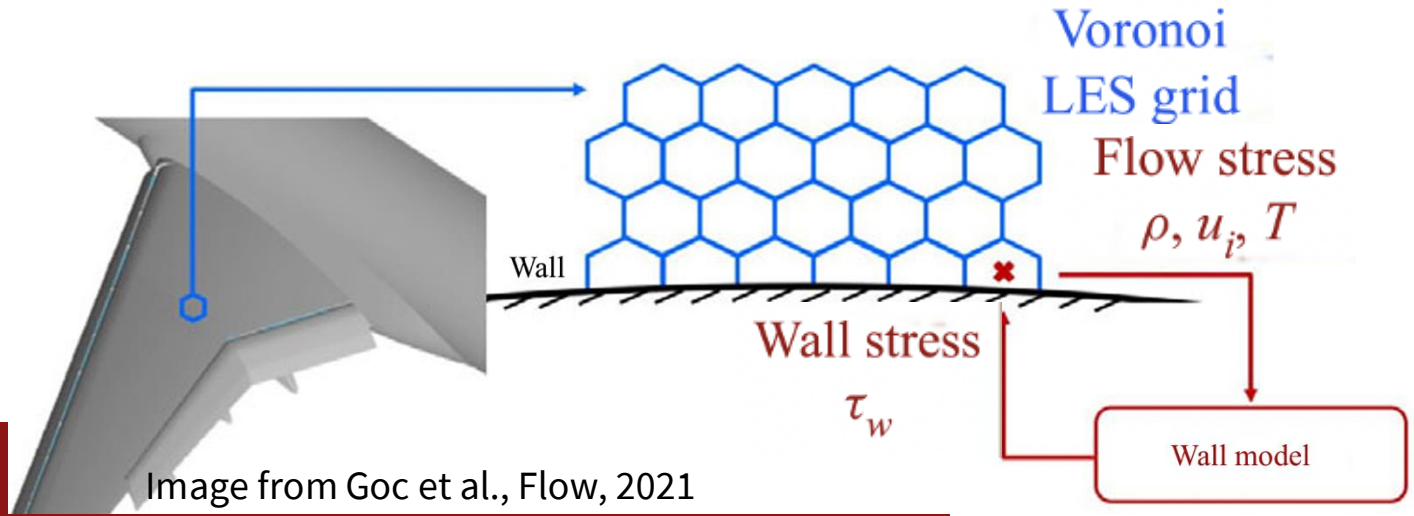
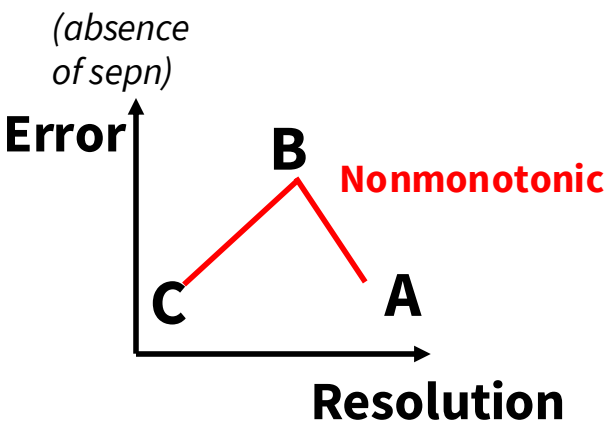


Image from Goc et al., Flow, 2021

1: Cabot and Moin, Flow Turb. Combustion, 2000

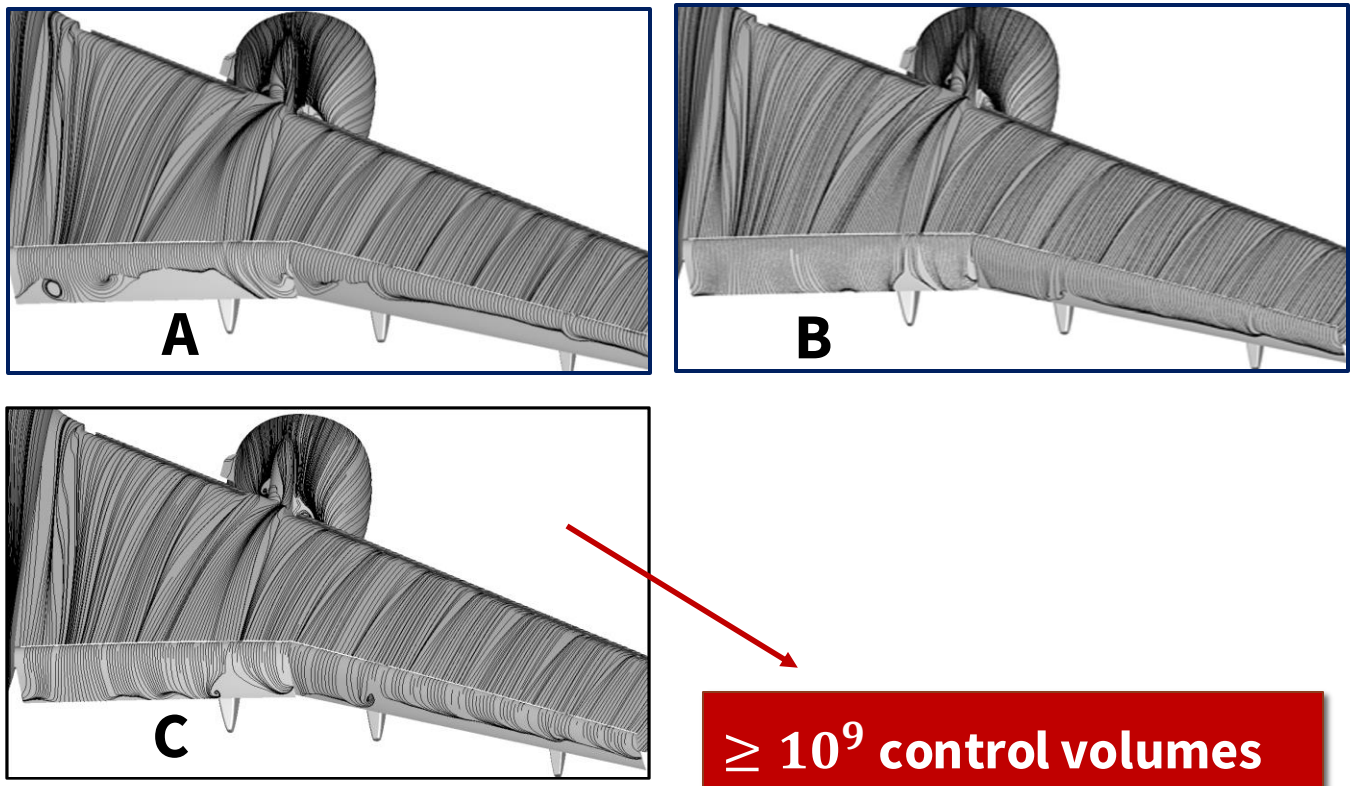
Recent observations from WMLES in separated flows: issue of non-monotonic grid convergence

Nonmonotonic grid convergence: a recent failure of Boussinesq models based WMLES in separated flows[1,2]



Improved models needed for reducing computational costs of wall-modeled LES of complex flows and to ensure monotonic approach toward expts!

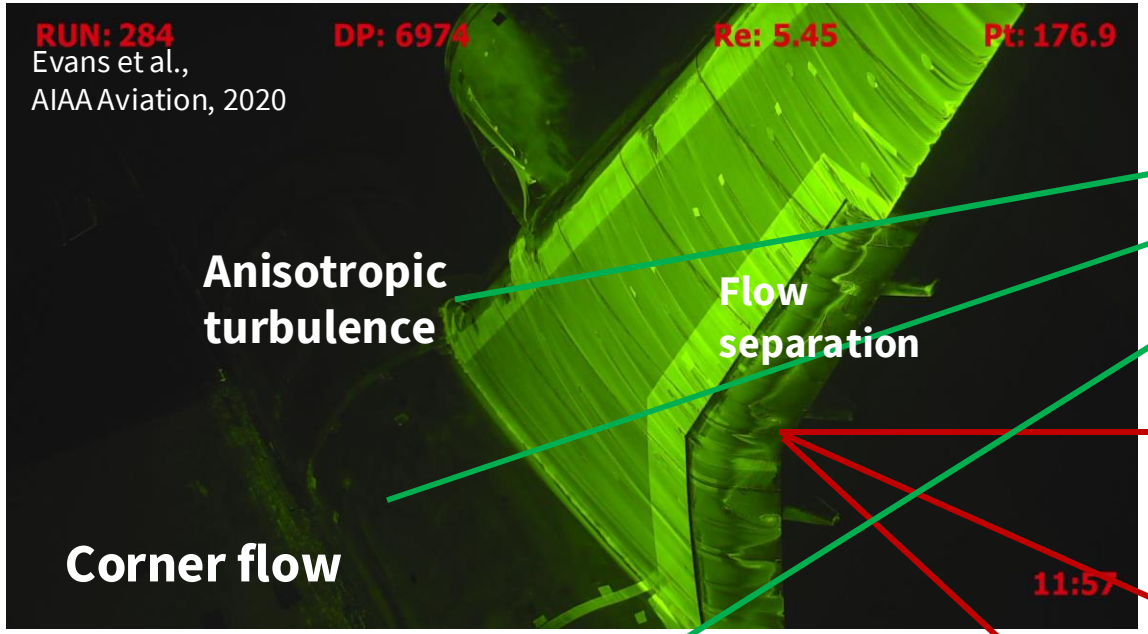
Flow over high-lift aircraft

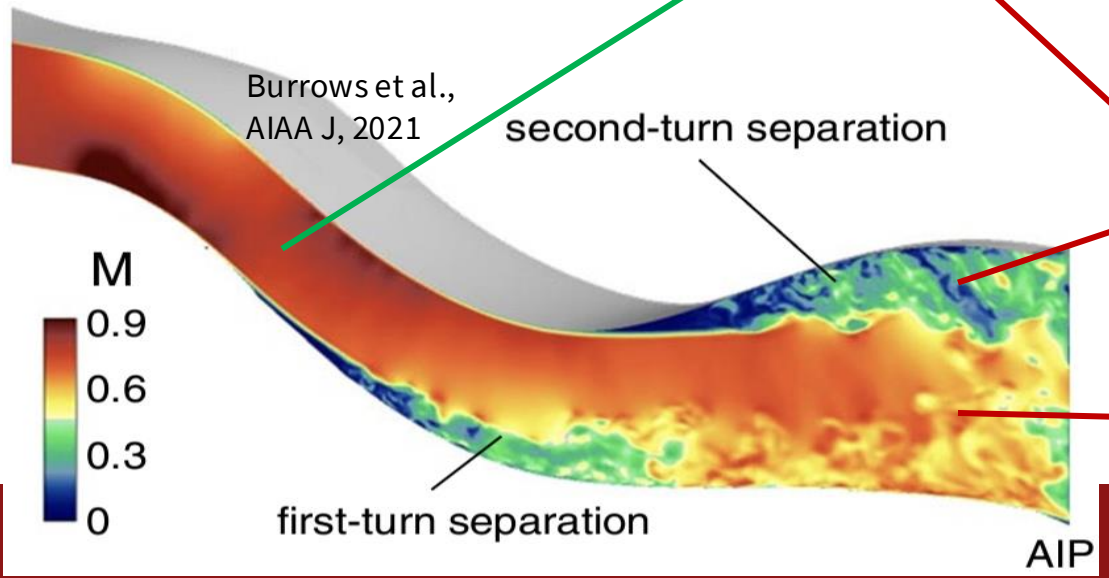


$\geq 10^9$ control volumes

1: Goc et al., Flow, 2021
2: Goc et al., J. Aircraft, 2023

Outline of this thesis





Alleviation of the Boussinesq hypothesis in SGS modeling

Grid point scaling of WMLES of separated boundary layers

Sensor based wall model for predicting smooth-body separation

WMLES of complex engineering flows underdoing separation

Alleviating the eddy viscosity assumption: Dynamic Tensor Coefficient Smagorinsky Model (DTCSM)[1]

- Aimed at reducing the misalignment problem of subgrid-stresses and strain rates.

- Anisotropic directional dependence:

$$\tau_{ij}^{sgs} - \frac{1}{3}\delta_{ij}\tau_{kk}^{sgs} = -\left(C_{ik}S_{kj} + C_{jk}S_{ki}\right)|S|\Delta^2$$

No assumption of alignment b/w τ_{ij}, S_{ij}

- **Extension of dynamic procedure with realizability constraints leads to**

(1) $C_{11} = C_{22} = C_{33}$. **(2)** $C_{ij} = -C_{ji}$ **when** $i \neq j$

Dissipative part **Non-dissipative part**

$$L_{ij} = \widehat{\bar{u}_i\bar{u}_j} - \hat{\bar{u}}_i\hat{\bar{u}}_j \text{ and } M_{ij} = \left(\frac{\hat{\Delta}}{\Delta}\right)^2 \widehat{|\bar{S}|\bar{S}_{ij}} - \widehat{|\bar{S}|\bar{S}_{ij}}$$

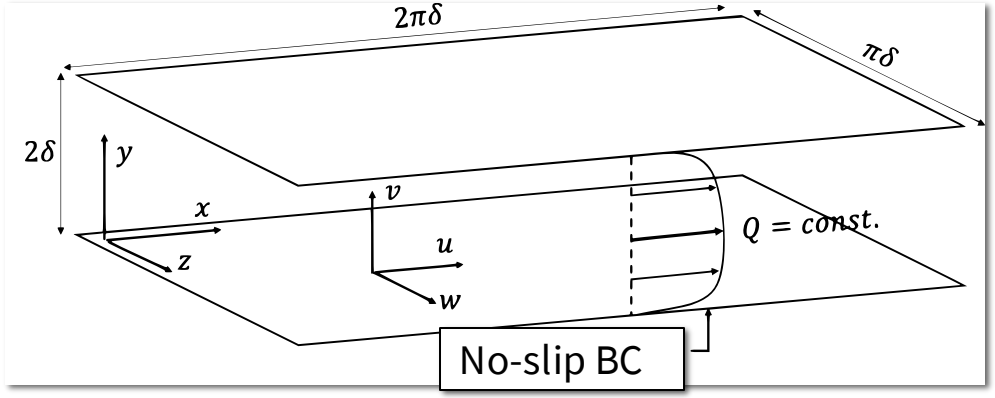
$$\begin{pmatrix} L_{11} \\ \end{pmatrix} \quad \begin{pmatrix} 2M_{11} & 2M_{12} & 2M_{13} & 0 \\ \end{pmatrix}$$

Sanity checks

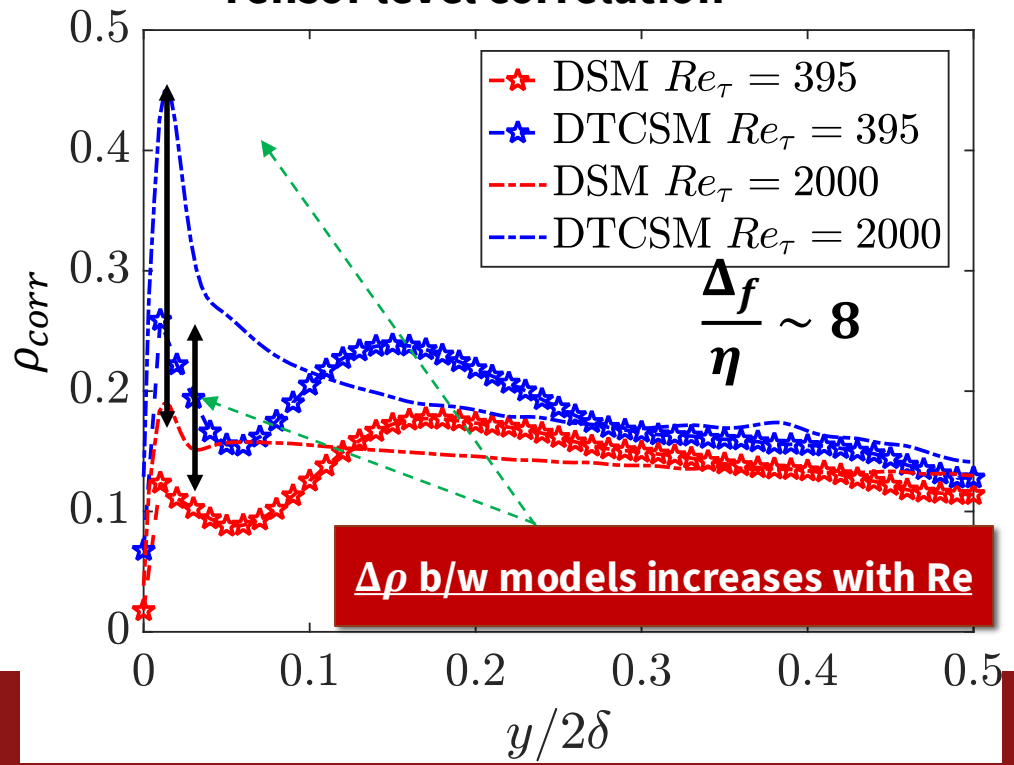
1) *a-priori* correlations?
2) Can this "dynamic" model adequately dissipate energy?
3) Can we predict canonical attached wall bounded flow?

1: Agrawal et al., Phys. Rev. Fluids, 2022

Apriori correlations in turbulent channel flows at $Re_\tau = 395, 2000$

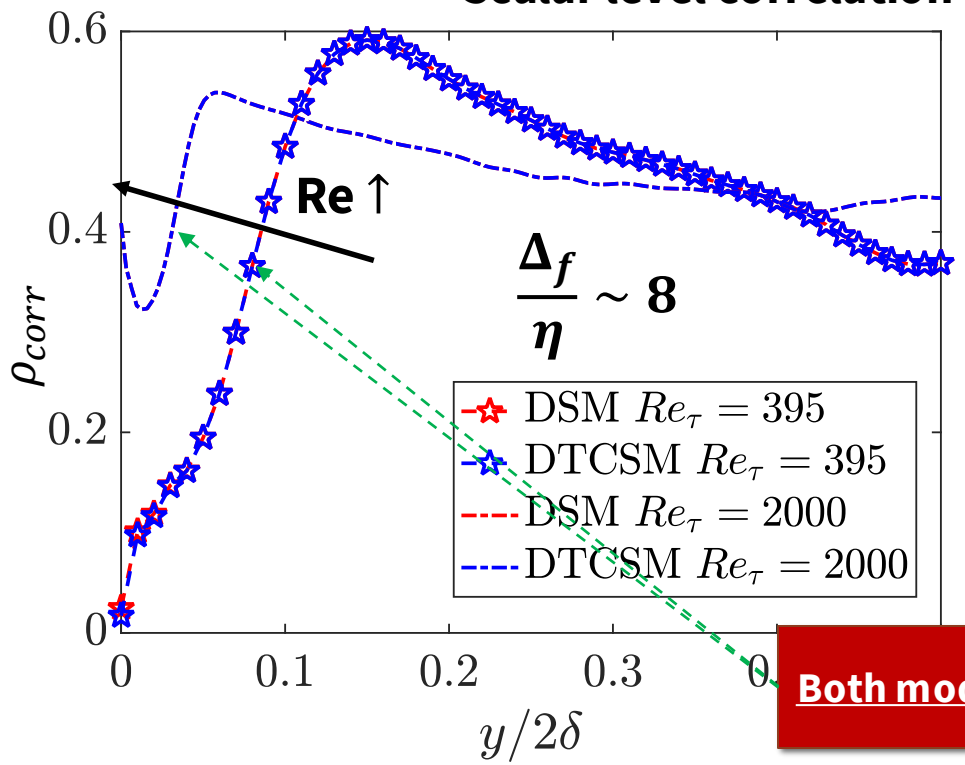


Tensor level correlation



Δρ b/w models increases with Re

Scalar level correlation



Both models dissipate equally

Our computational approach

- ***charLES*** flow solver
  - 2nd order finite-volume method
  - Skew symmetric ops.: low-dissipation numerics
  - GPU accelerated version

$$\frac{\partial \bar{\rho}}{\partial t} + \frac{\partial \bar{\rho}\widetilde{u_j}}{\partial x_j} = 0$$

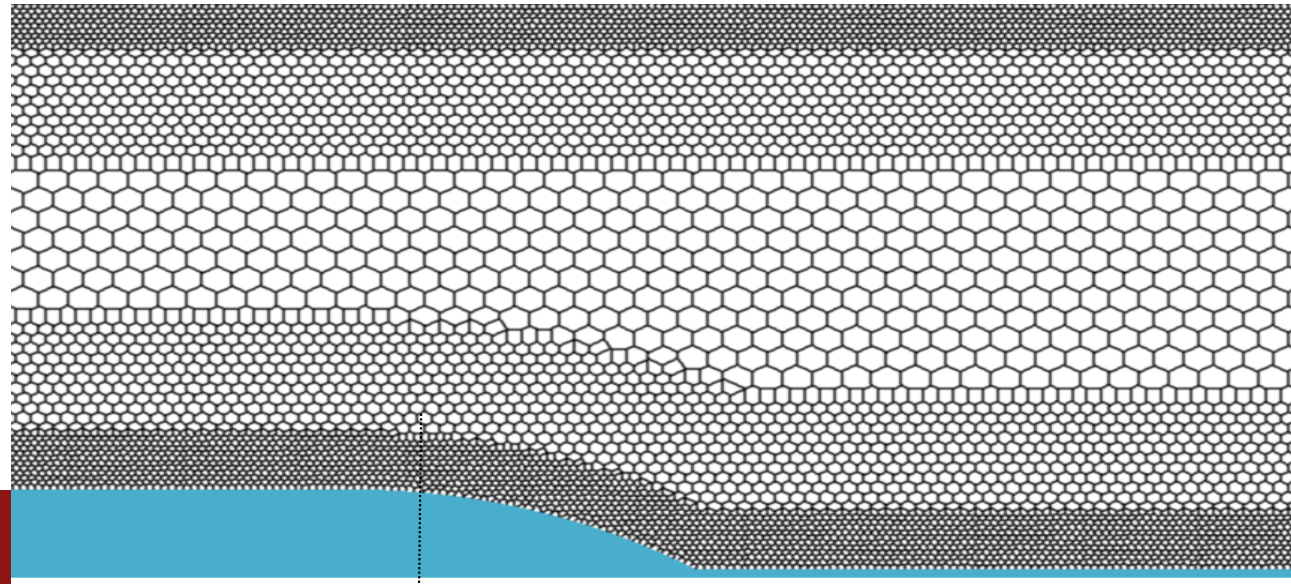
Subgrid-scale model: needs modeling

$$\frac{\partial \bar{\rho}\widetilde{u_i}}{\partial t} + \frac{\partial \bar{\rho}\widetilde{u_i}\widetilde{u_j}}{\partial x_j} + \frac{\partial \bar{p}}{\partial x_i} = \frac{\partial \widetilde{\sigma_{ij}}}{\partial x_j} - \frac{\partial \boldsymbol{\tau_{ij}^{SGS}}}{\partial x_j}$$

Subgrid heat flux: needs modeling

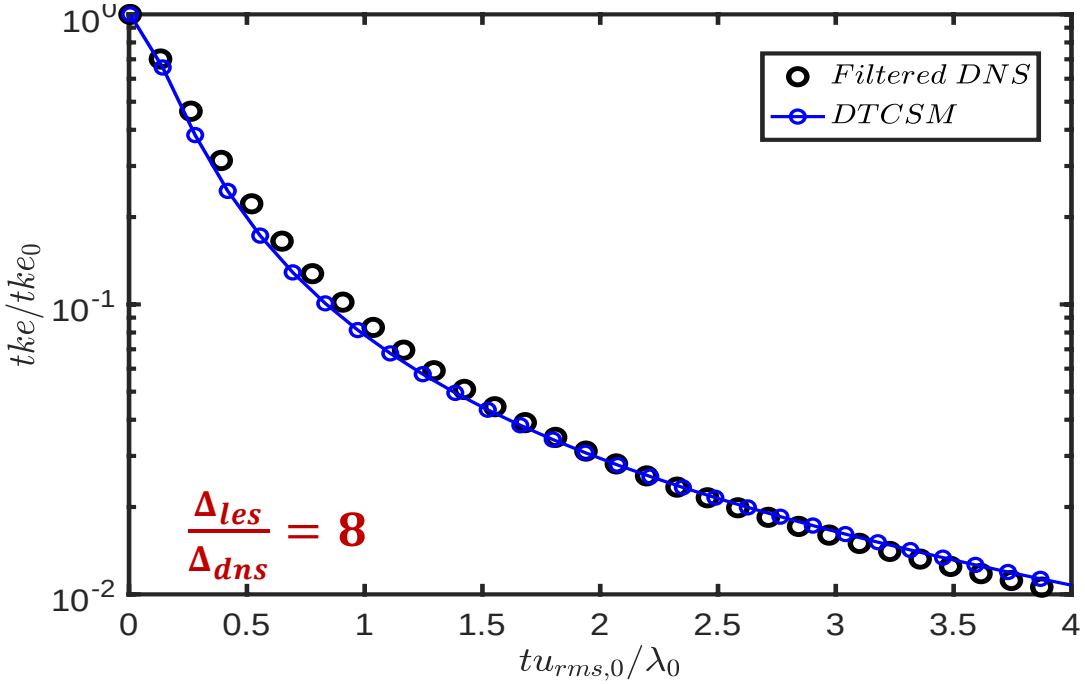
$$\frac{\partial \bar{E}}{\partial t} + \frac{\partial\left[(\bar{E}+\bar{p})\widetilde{u_j}\right]}{\partial x_j} = \frac{\partial}{\partial x_j}\left(\frac{k\partial \bar{T}}{\partial x_j}\right) + \frac{\partial\left(\widetilde{u_i}\widetilde{\sigma_{ij}}\right)}{\partial x_j} - \frac{\partial \boldsymbol{Q_j^{SGS}}}{\partial x_j} - \frac{\partial\left(\widetilde{u_i}\tau_{ij}^{SGS}\right)}{\partial x_j}$$

- Meshing based on Voronoi tessellations
  - Hexagonal close-packed topology
  - Near-wall refinement

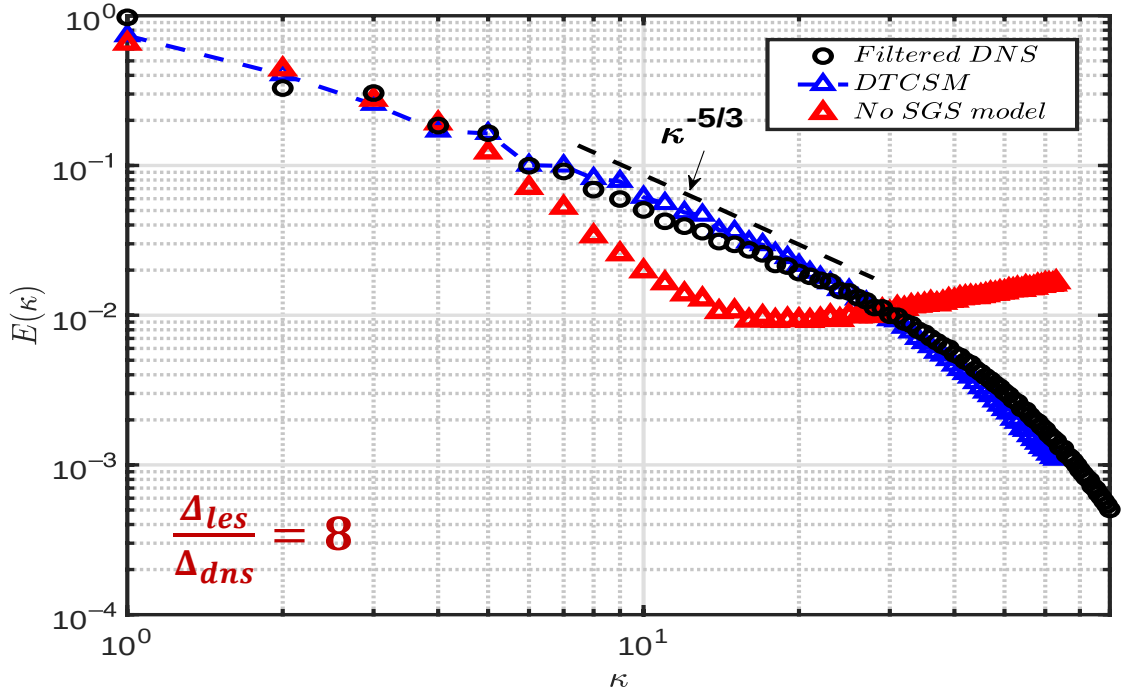


A-posteriori validation case I: Isotropic turbulence at Re_λ = 70 and 315

$Re_\lambda = 70$: Kinetic energy vs time

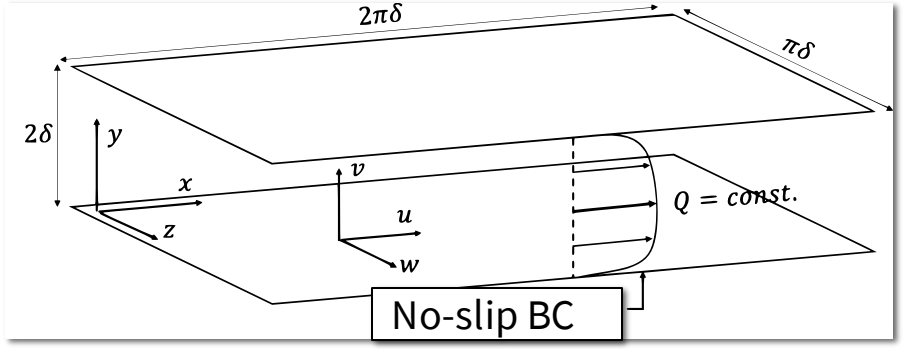


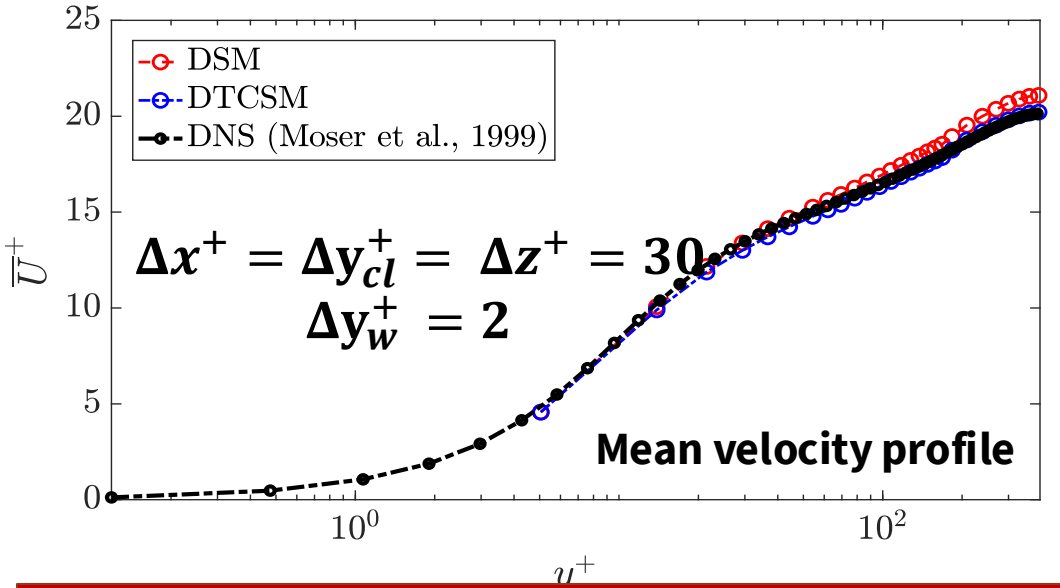
$Re_\lambda = 315$: Kinetic energy spectrum

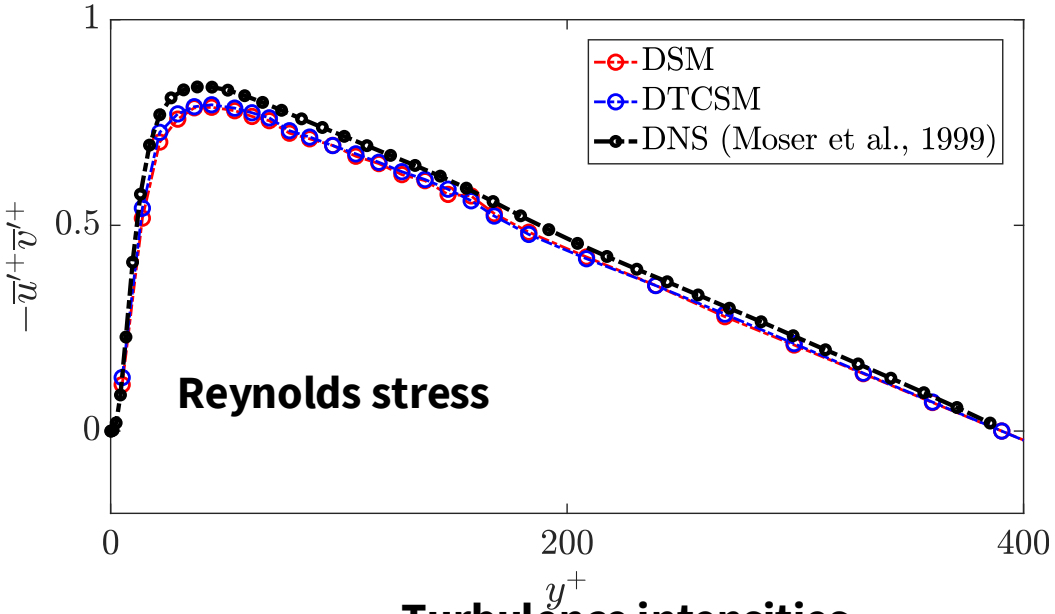


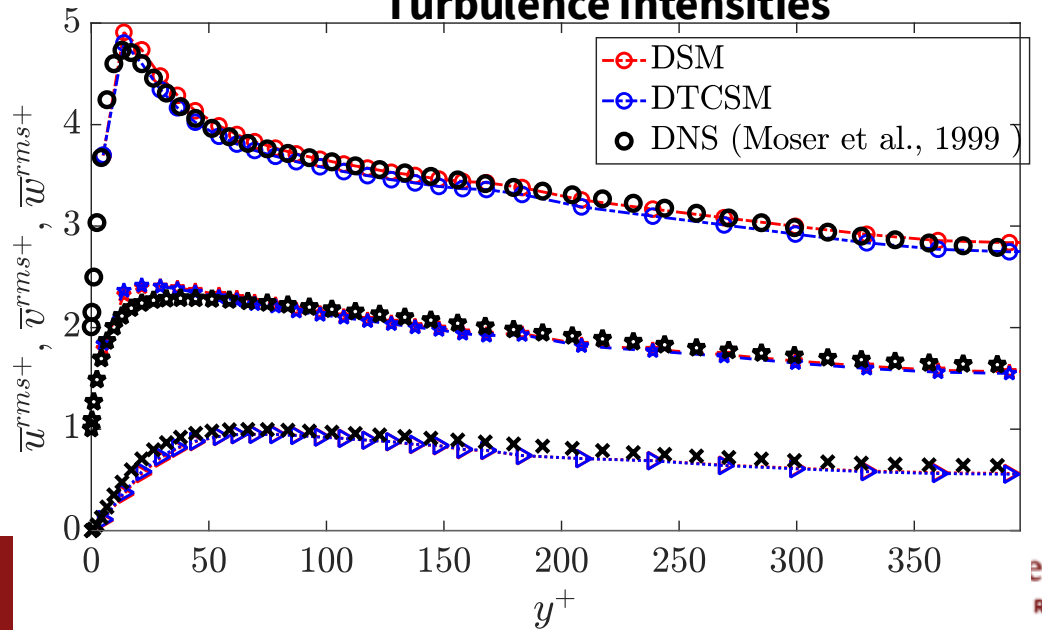
- **DTCSM is comparably dissipative to DSM; and produces reasonable energy spectra**
- Several previous non-Boussinesq models have been under dissipative, and unstable
  - **Bardina model (1980), Gradient model (1979)**
  - ***A priori correlations* > *80*%,** but underdissipative a-posteriori.

Validation case II: Wall-resolved LES of a channel flow at $Re_\tau = 395$





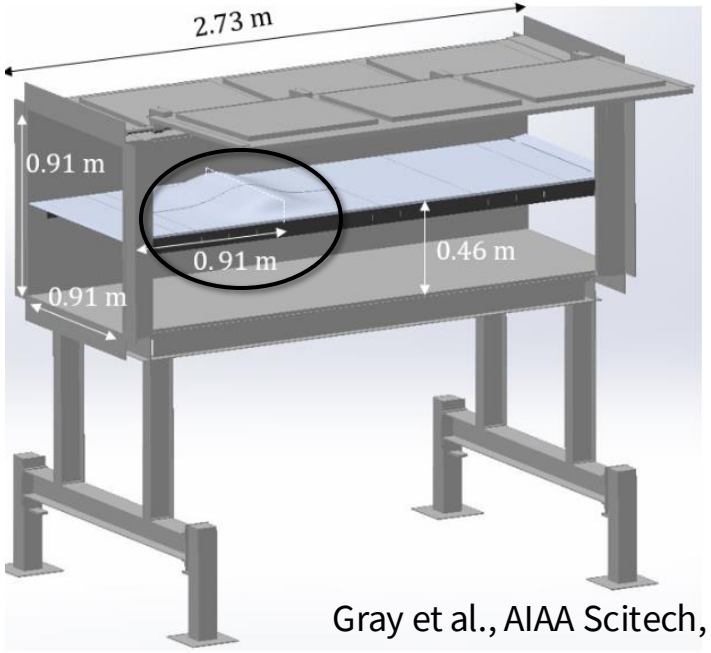




DTCSM accurately predicts first and second order statistics in a low Re channel flow

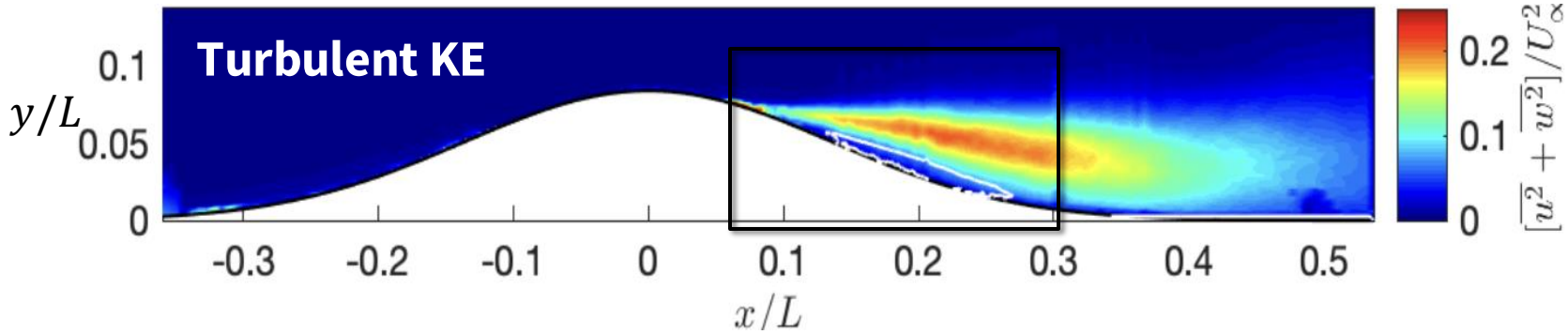
Validation case III: Smooth body separation on the Boeing speed bump

- Recently designed canonical flow configuration: **Boeing speed bump**
  - **Gaussian shaped streamwise body**
  - **Expts (shoulders tapered): Williams et al., Gray et al., AIAA Scitech, 2021**
  - Quasi DNS (spanwise-periodic): Uzun and Malik, AIAA J, 2021
  - $\boldsymbol{Re_L = \frac{U_\infty L}{\nu} = 2 \times 10^6}$

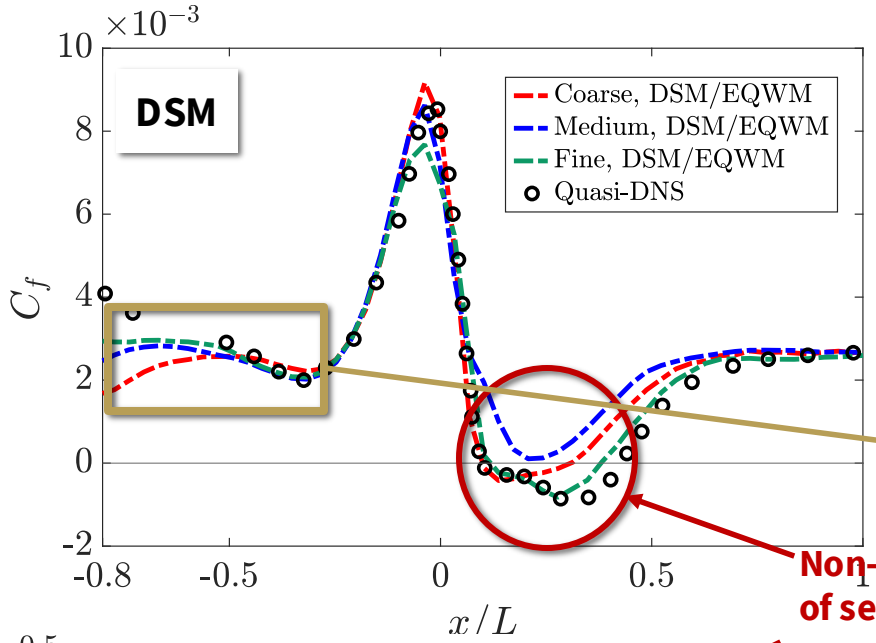


Gray et al., AIAA Scitech, 2021

$$y/L \sim \exp(-x^2/x_0^2)$$



Boeing speed bump – prediction of skin-friction and wall pressure

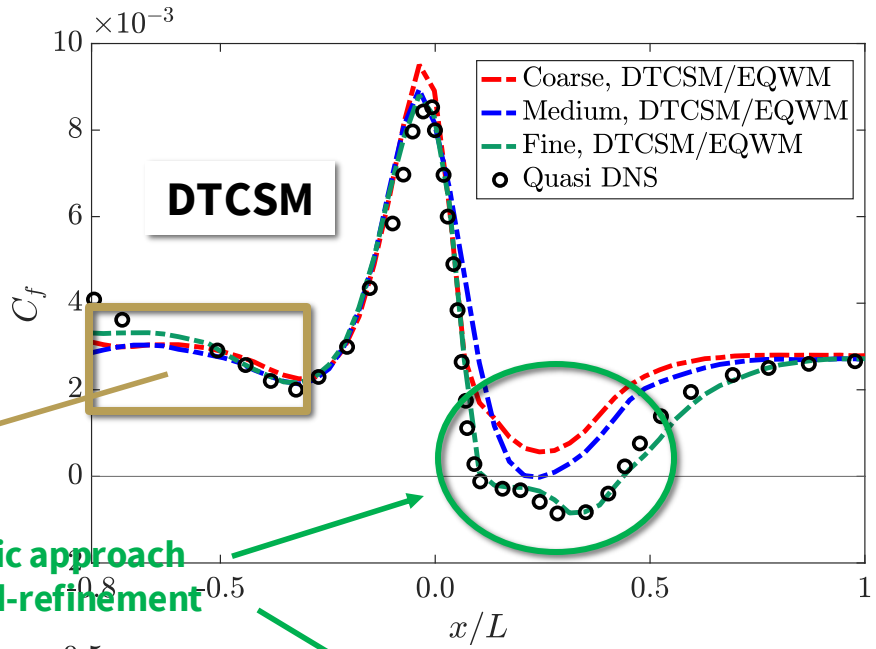


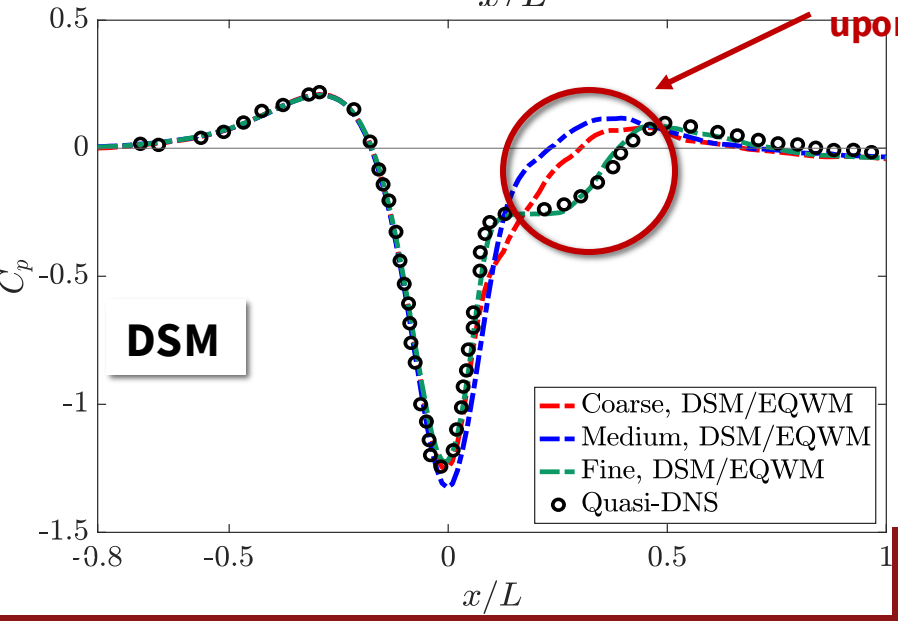
Skin-friction

ZPG development length smaller with DTCSM

Non-monotonic occurrence of separation bubble upon grid-refinement

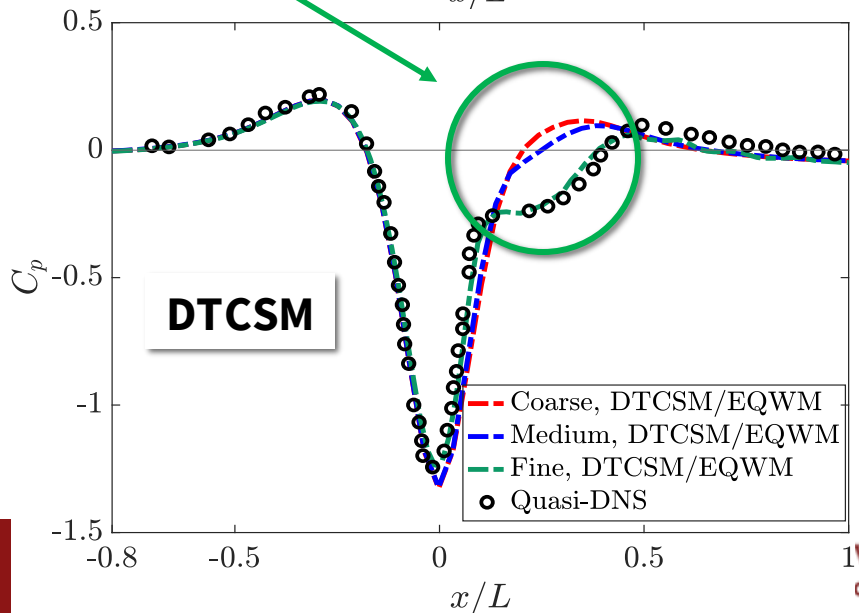
Monotonic approach upon grid-refinement





Wall-pressure

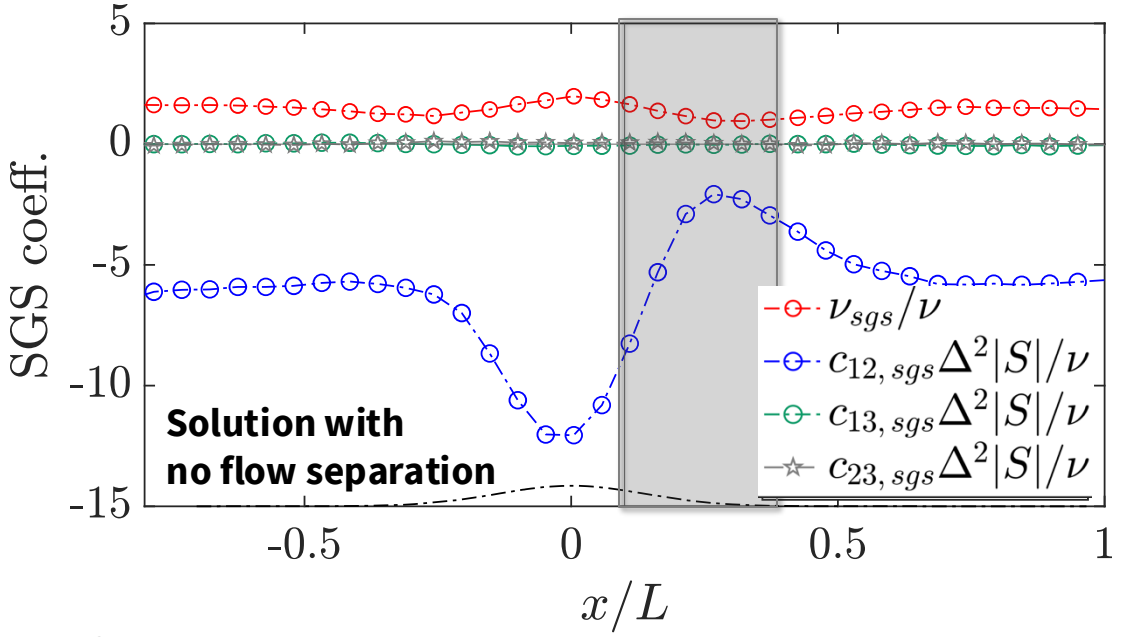
Coarse grid: 3 Mcv, avg(Δy_w^+) ~ 50
Medium grid: 12 Mcv, avg(Δy_w^+) ~ 25
Fine grid: 52 Mcv, avg(Δy_w^+) ~ 13
Quasi-DNS: 10 Bcv

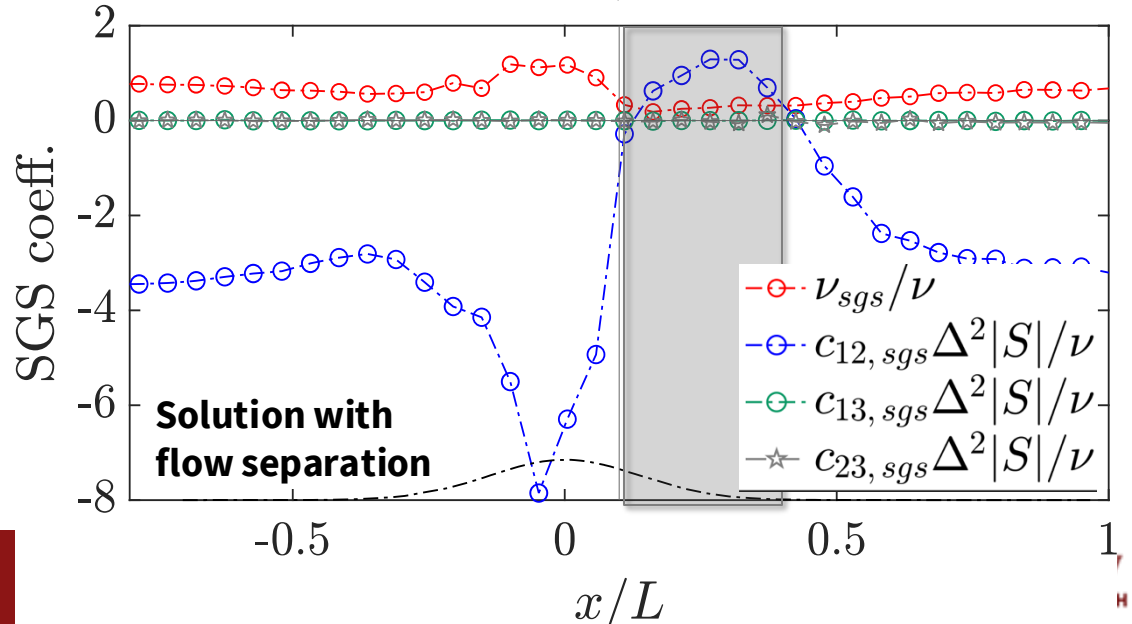


versity
CE RESEARCH

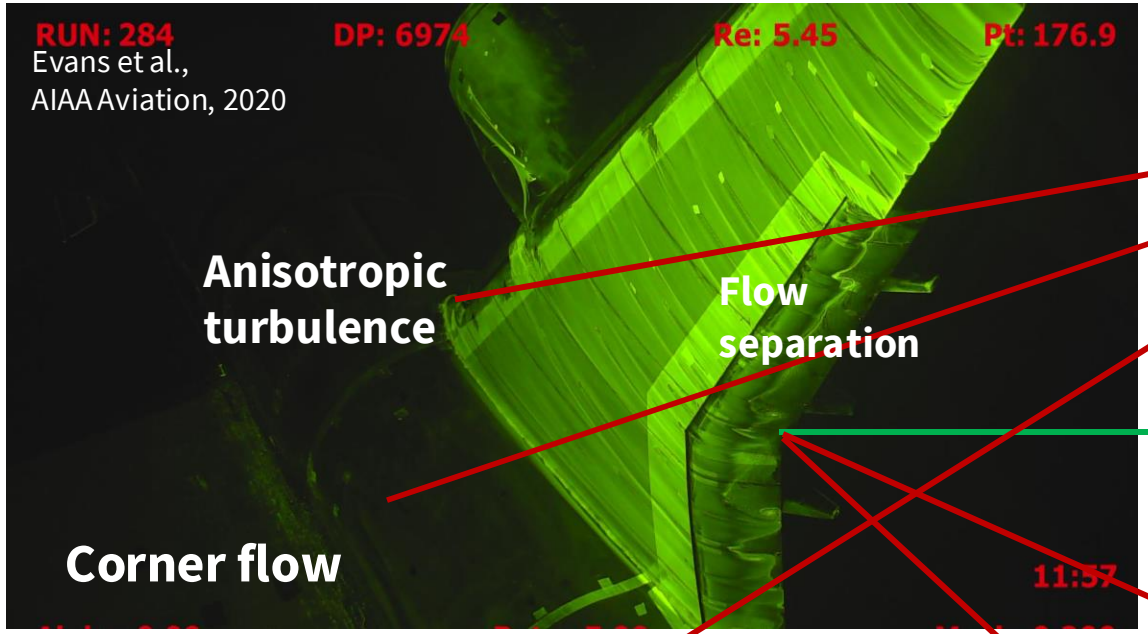
Boeing speed bump – distribution of near-wall SGS model coefficients

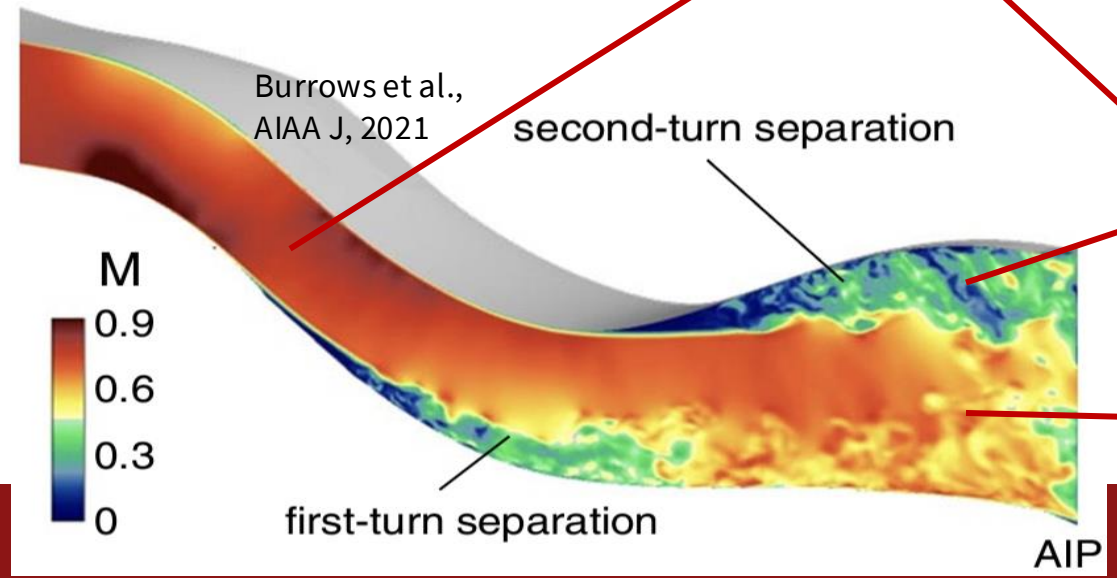
- **Mean value of c_{12} is at least comparable to ν_{sgs}, if not larger**
  - Mean c_{12} tracks with mean shear in 1-2 direction.
  - Always remains negative on med. grid, but switches sign when mean shear switches sign.
- **c_{13}, c_{23} are small in the mean for this flow**
  - No mean shear along periodic spanwise direction





Outline of this thesis





Alleviation of the Boussinesq hypothesis in SGS modeling

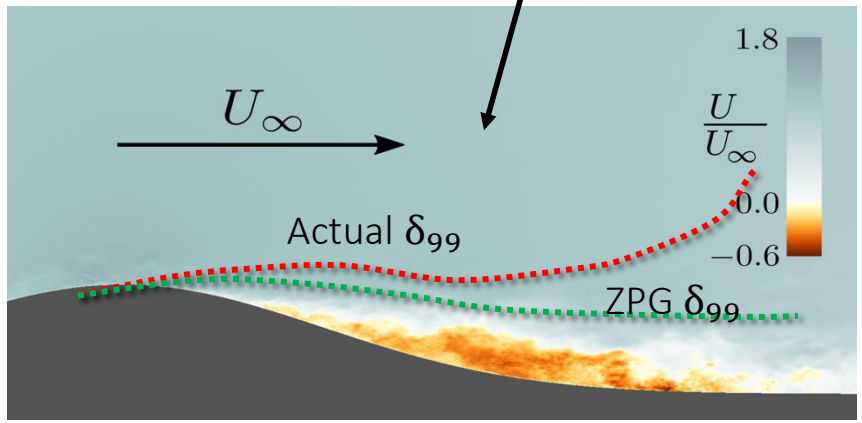
Grid point scaling of WMLES of separated boundary layers

Sensor based wall model for predicting smooth-body separation

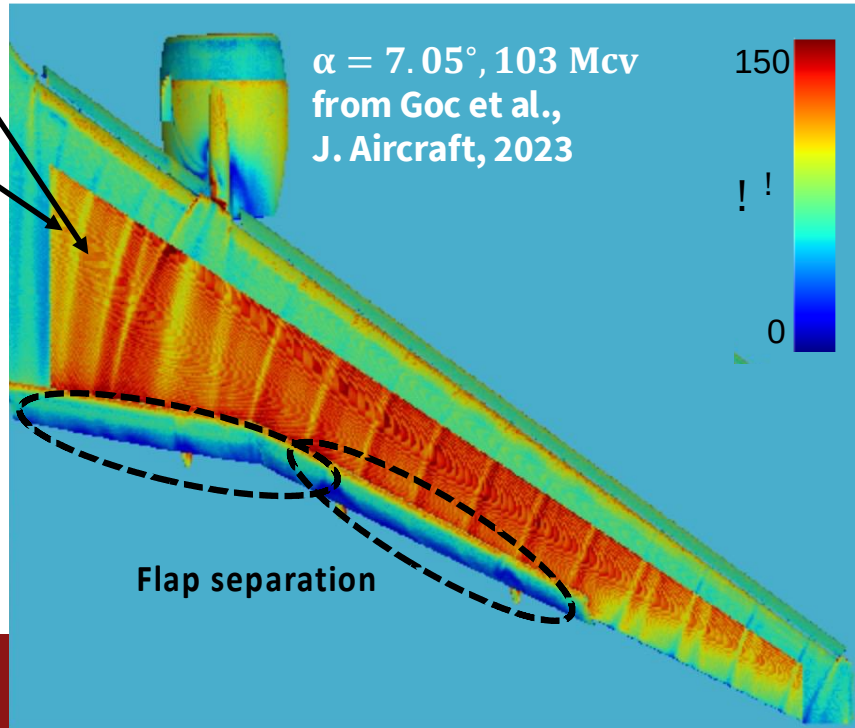
WMLES of complex engineering flows underdoing separation

Grid-point scaling (with Reynolds number) of WMLES of separated flows

- **Existing estimates[1,2] of grid-point estimates ($N_{cv} \sim Re^{1}$) rely on equilibrium phenomenology**
  - Use viscous resolution, y^+ to determine if grid-refinement is necessary
  - **Ignore QoI's dependence on resolution**
  - Ignore explicit dependence of δ on $\frac{dP}{dx}$

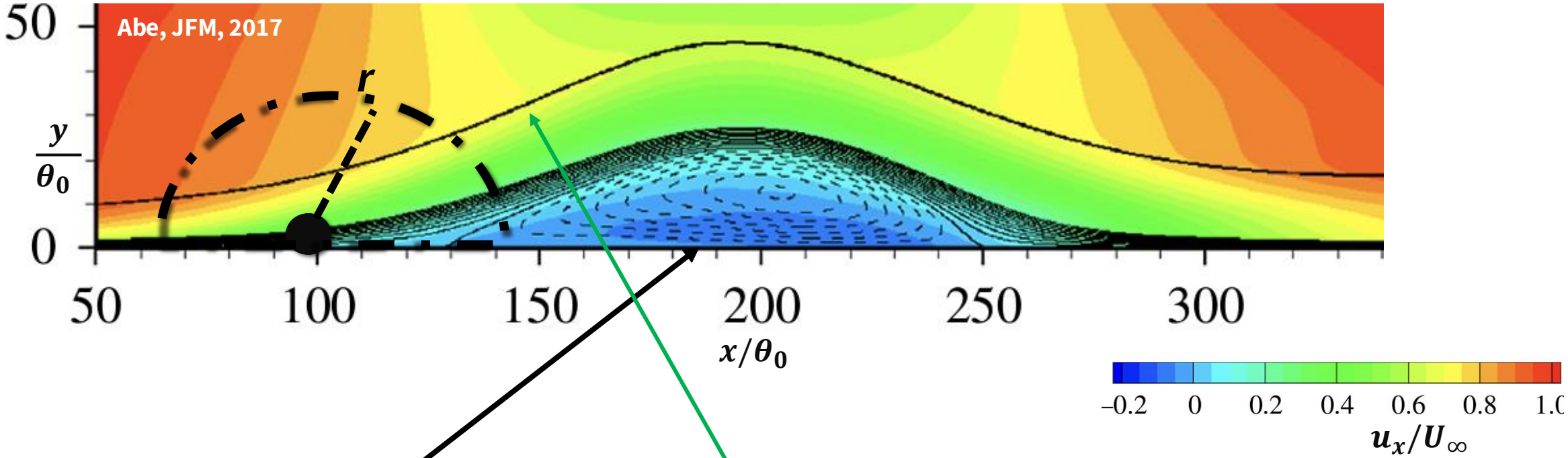


Where to target grid-refinement to improve C_L prediction?



1. Choi and Moin, *Phys. Fluids*, 2012
2. Yang and Griffin, *Phys. Fluids*, 2021

Separating flow over flat-plate: region of influence around separation pt.



Separation point over a flat-plate

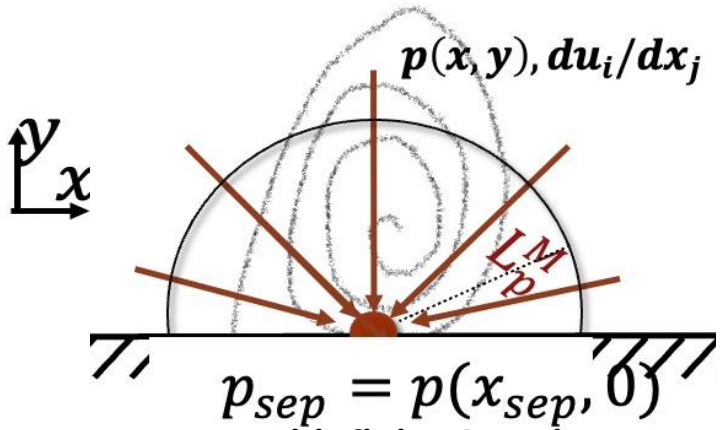
Near-wall equilibrium region that affects the separation point?

Green's function approach to determine equilibrated flow-scales

- Solve the **Poisson** system, $\left\langle \rho \frac{\partial \overline{u_i}}{\partial x_j} \frac{\partial \overline{u_j}}{\partial x_i} \right\rangle = -\nabla^2 \langle \overline{p} \rangle$ in a semi-infinite domain

$$\langle p^*_{sep} \rangle = -\int_{y^* \geq 0} \int_{x^* \in R^1} \frac{log\left(r^{*2}\right)}{2\pi} \left\langle \rho \frac{\partial \overline{u_i^*}}{\partial x_j^*} \frac{\partial \overline{u_j^*}}{\partial x_i^*} \right\rangle dx^* dy^*$$

r^* = distance from separation point, quantities non dimensionalized by $u_p^3 = min(\frac{\nu}{\rho}\frac{dP}{dx})$ and $l_p = \frac{\nu}{u_p}$)



Semi-infinite domain approximation for a flat-plate separating BL

- For a "**finite sphere of influence**" assumption at the separation point, $\frac{log\left(r^{*2}\right)}{2\pi} \left\langle \rho \frac{\partial \overline{u_i^*}}{\partial x_j^*} \frac{\partial \overline{u_j^*}}{\partial x_i^*} \right\rangle \leq \Lambda^2, \ \Lambda \in R^1$

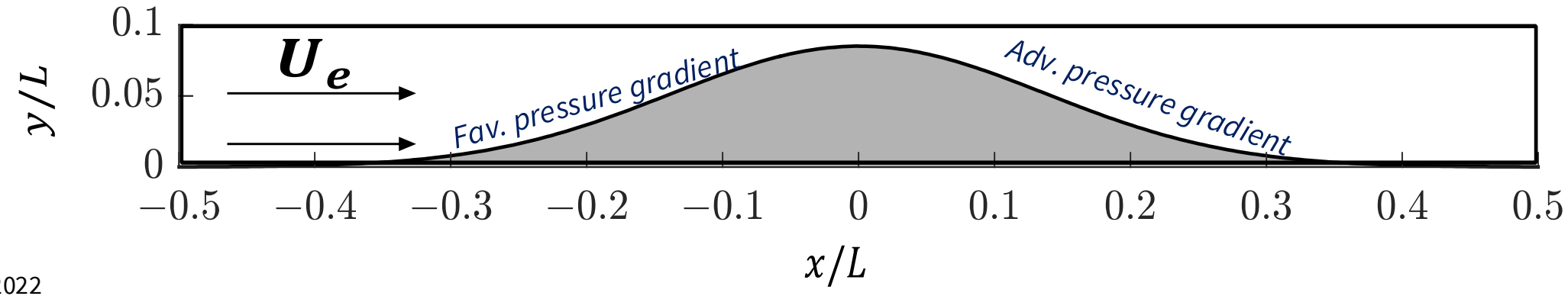
- Invoke Stratford's[1] velocity profile for a separating flow to arrive at $r^* \sim \Lambda\, l_p \sim Re_p^{-2/3}$

For nested grids, $N_{pts} \sim \frac{1}{r^2} \sim Re_p^{4/3} \Rightarrow N_{pts} \sim Re_p^{>1}$

1. Stratford, *JFM*, 1959

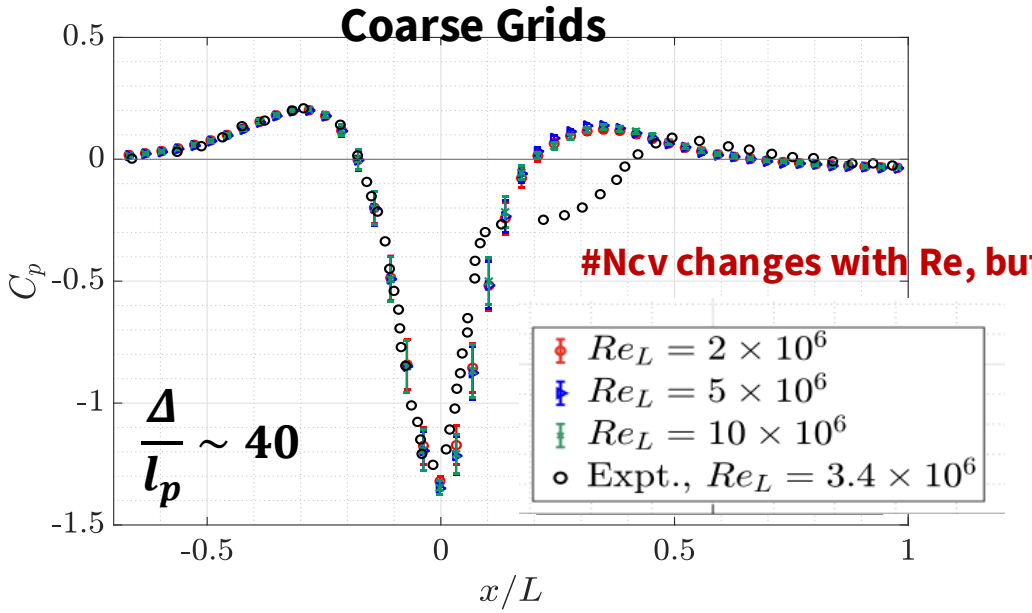
Proof of concept on the Boeing speed bump

- Experiments of Gray et al: approximately Reynolds number invariant separation profile (C_p)
- In WMLES, we increase Reynolds number from 2×10^6 up to 10×10^6
  - Grid refinement per $\Delta \sim Re^{-2/3}$ metric
  - If C_p across multiple Re agree with reference data at a fixed $\frac{\Delta}{l_p}$, then the hypothesis is verified.

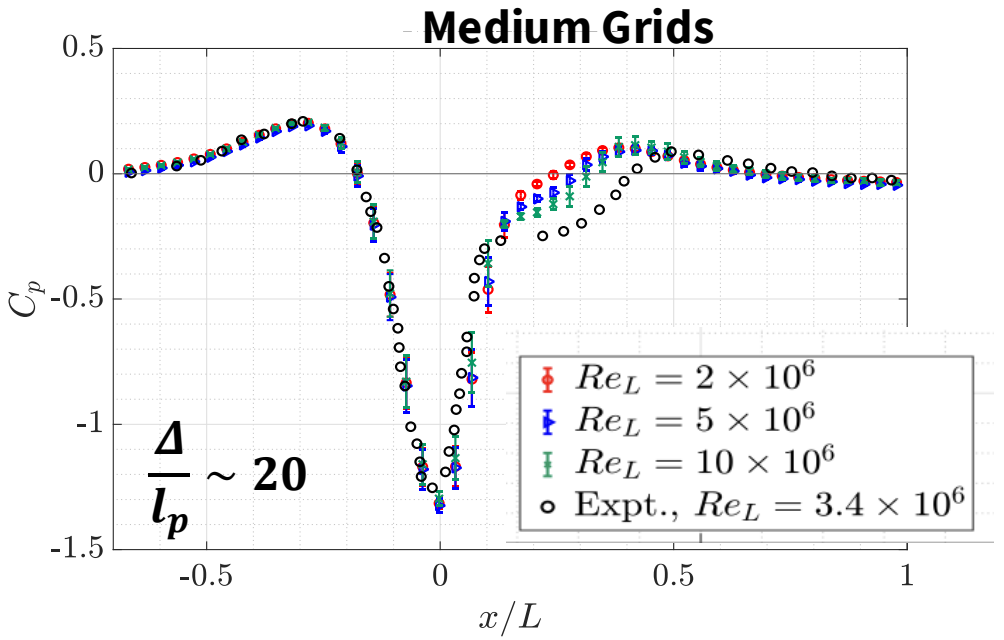


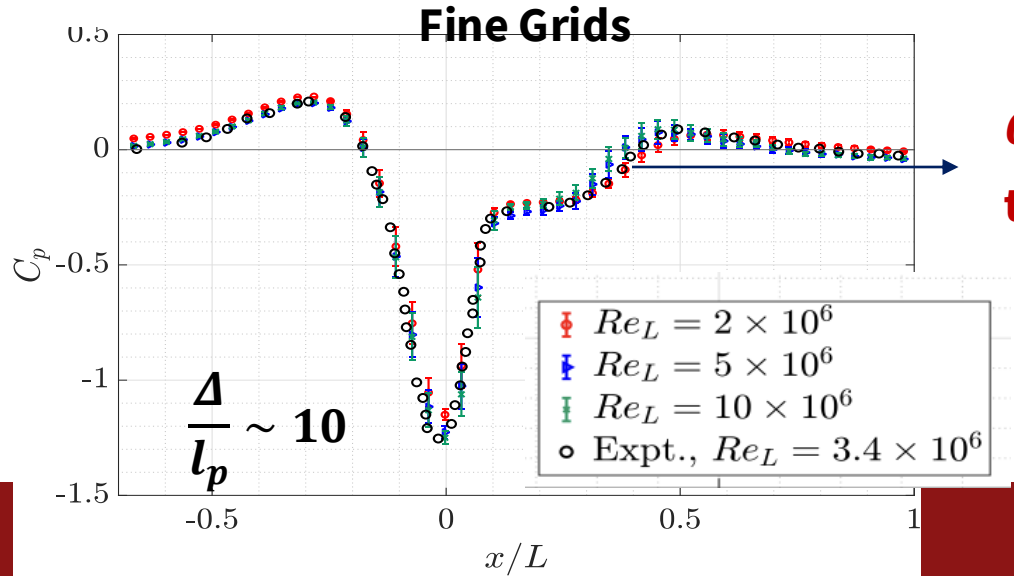
1: Gray et al., *AIAA* 2022

For increasing Re, when grids are refined such that $\Delta/l_p \neq f(Re)$, WMLES converges to reference data for a constant value of Δ/l_p



#Ncv changes with Re, but at the same $\frac{\Delta}{l_p}$





C_p across multiple Re converge toward expts. at fixed $\frac{\Delta}{l_p}$

Grid counts for $Re_L = 2 \times 10^6$ case

Coarse grid: 3 Mcv

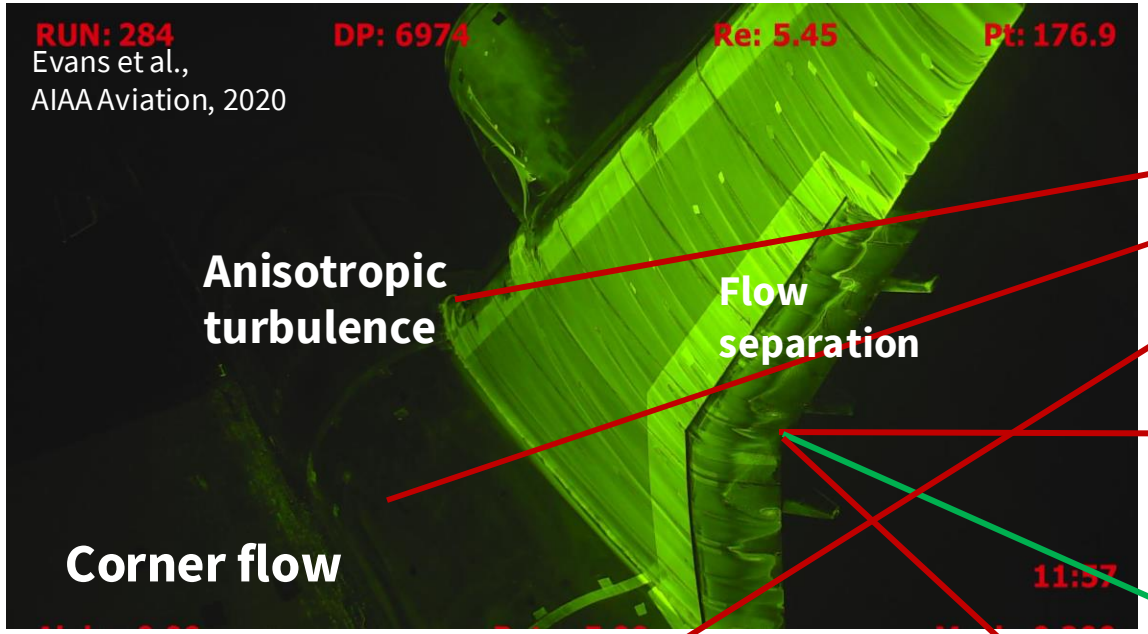
Medium grid: 12 Mcv

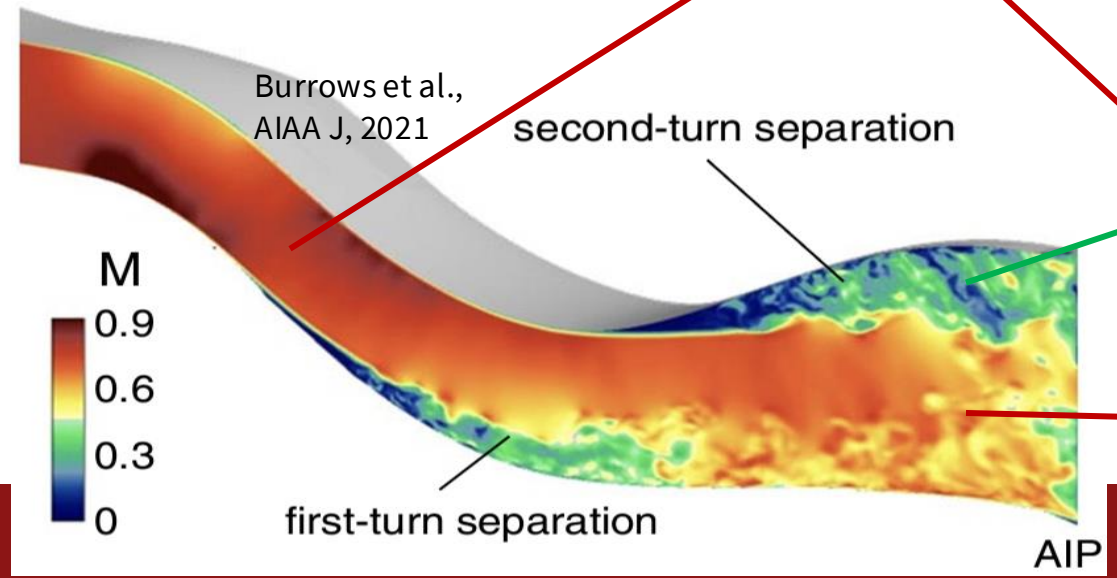
Fine grid: 52 Mcv

Quasi-DNS: 10 Bcv

*All cases were simulated using DTCSM/EQWM

Outline of this thesis





Alleviation of the Boussinesq hypothesis in SGS modeling

Grid point scaling of WMLES of separated boundary layers

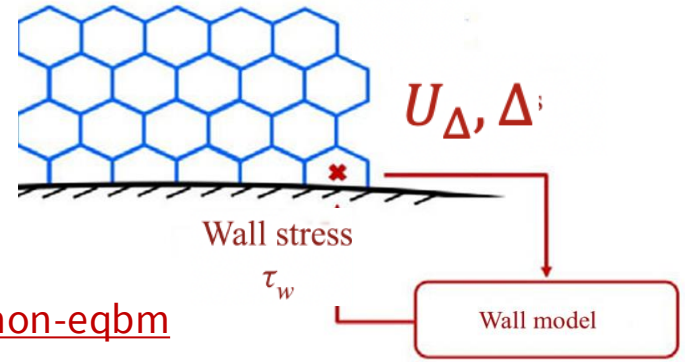
Sensor based wall model for predicting smooth-body separation

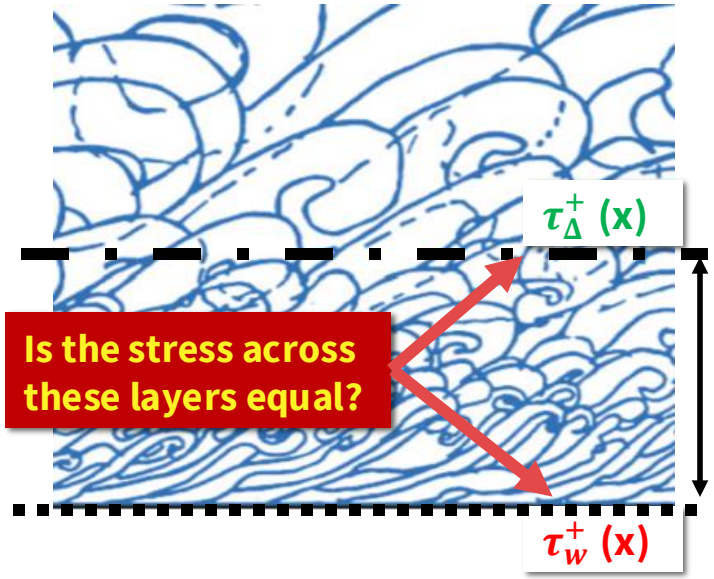
WMLES of complex engineering flows underdoing separation

Nonequilibrium effects in turbulent boundary layers

- Due to a pressure gradient, the boundary layer suffers "history effects[1]"
  - *Local* Reynolds number, pressure gradient is incomplete representations of flow state.

- Lagrangian integration of Navier-stokes equations





$$\frac{\int_0^{x^+} \tau_\Delta^+ dx^+}{\int_0^{x^+} \tau_w^+ dx^+} \approx 1 + \frac{\int_0^{x^+}\int_0^{\Delta^+} \left[\frac{u_p^3}{u_\tau^3} + u^+\frac{du^+}{dx^+} + v^+\frac{du^+}{dy^+}\right] dy^+ dx^+}{\int_0^{x^+} dx^+}$$

$\mathcal{H}(x^+)$: local measure of non-eqbm

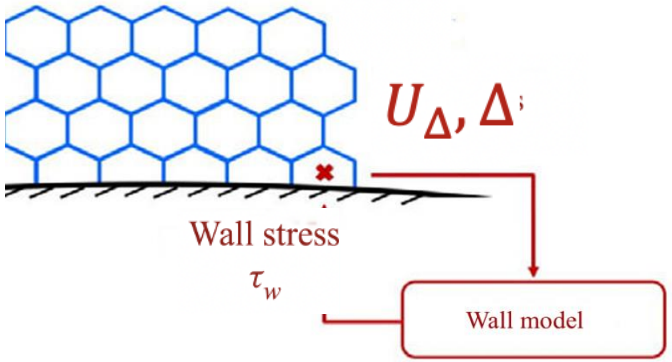
where $u_p^3 = \frac{\nu}{\rho}\frac{dP}{dx}$, $u_\tau^2 = \frac{\tau_w}{\rho}$

If $\mathcal{H}(x^+) \approx 0 \Rightarrow \int_0^{x^+} \tau_\Delta^+ dx^+ \approx \int_0^{x^+} \tau_w^+ dx^+$, or a constant stress layer holds across the flow up to height Δ^+

1. Bobke et al., J. Fluid Mech., 2017

Determination of imminent separation tendency of a given boundary layer

- Alber's parameter[1], $\Lambda = \frac{\theta}{\rho U_e^2}\frac{dP}{dx}$: outer measure of impending flow separation.
  - Alber (1971): $\Lambda \geq 0.004$, flow close to imminent separation[1,2]



- A linear Taylor's series expansion of the **Von-Karman integral momentum balance** for attached boundary layers can be shown to follow[2]

$$\frac{C_f}{2} \approx \frac{C_c}{2Re_\theta} + \frac{C_{Re,\infty}}{2} + \left[\frac{C_m}{2} - 2 - \frac{\delta^*}{\theta}\right]\frac{\theta}{\rho U_e^2}\frac{dP}{dx}$$

model coefficients of linear Taylor series expansion

Λ

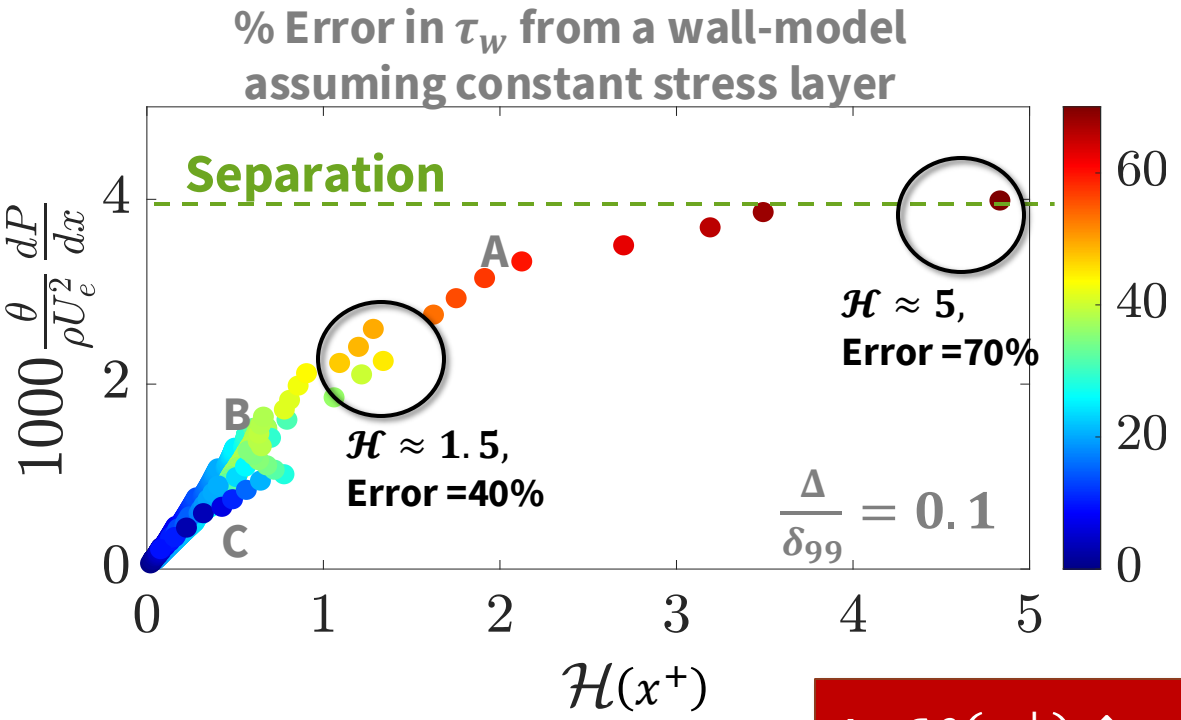
In limit of high Re_θ, for an impending sepn. ($C_f \approx 0$), Λ describes proximity to onset of sepn.

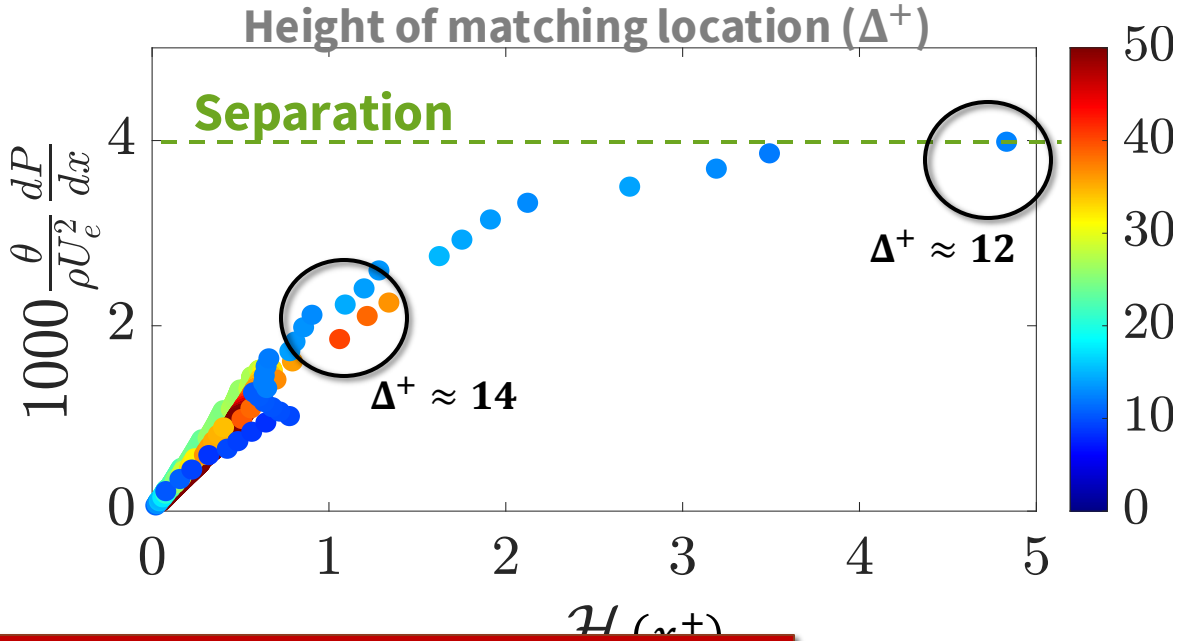
1: Alber, Aerospace Sci. Meeting, 1971
2. Agrawal et al., Flow, 2024

Constant stress layer closure breaks down with increasing $\mathcal{H}$

$\mathcal{H}(x^+) = \int_0^{\Delta^+} \left[\frac{u_p^3}{u_\tau^3} + u^+\frac{du^+}{dx^+} + v^+\frac{du^+}{dy^+}\right] dy^+$: local measure of non-eqbm

$\Lambda = \frac{\theta}{\rho U_e^2}\frac{dP}{dx} y^+$: measure of separation





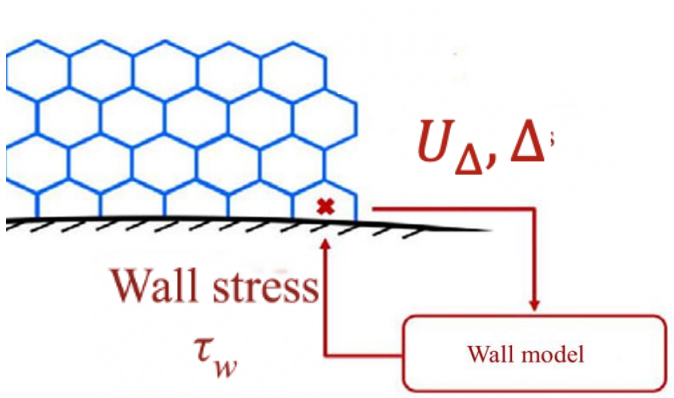
A, B, C denote different BLs in Bobke et al., JFM, 2017, and NACA4412 in Tanarro et al., JFM, 2020

As $\mathcal{H}(x^+)$ ↑, modeling errors significantly increase even for a "small" matching location

Opportunity: Can we use $\mathcal{H}$ to detect non-eqbm. near separation?

- Consider $\mathcal{H}$ again,

$$\mathcal{H}(x^+) = \int_0^{\Delta^+} \left[\frac{u_p^3}{u_\tau^3} + u^+\frac{du^+}{dx^+} + v^+\frac{du^+}{dy^+}\right] dy^+ \qquad u_p^3 = \frac{\nu}{\rho}\frac{dP}{dx} \text{ and } u_\tau^2 = \frac{\tau_w}{\rho}$$



- Kamogawa and Kawai, *Phys. Rev. Fluids*, 2023 provide a model closure for the convective terms as

$$u^+\frac{du^+}{dx^+} + v^+\frac{du^+}{dy^+} \approx \frac{u_p^3}{u_\tau^3}\left[\frac{\int_0^\Delta u^2\, dy}{U_\Delta^2\,\Delta}\right]$$

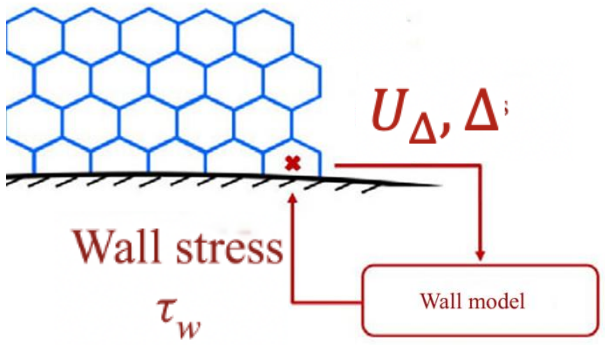
- Using this model form, and performing algebra to bound the integral in $\mathcal{H}$ leads to:

When $\frac{u_p^3}{u_\tau^3} \sim O(1)$, $\mathcal{H}$ becomes non-negligible

Thus, when $\frac{u_p^3}{u_\tau^3} > 1$, we consider flow non-equilibrium sensor to be active.

Pressure-gradient, convective terms inclusive wall-stress augmentation

- **Time-averaged form of LES equations** under the thin-boundary layer approximation:



$$\langle\overline{u_s}\rangle\frac{\partial\langle\overline{u_s}\rangle}{\partial s}+\langle\overline{u_n}\rangle\frac{\partial\langle\overline{u_s}\rangle}{\partial n}=-\left\langle\frac{\partial\overline{P}}{\partial s}\right\rangle+\nu\frac{\partial^2\langle\overline{u_s}\rangle}{\partial n^2}-\left\langle\frac{\partial\overline{u_s}'\overline{u_n}'}{\partial n}\right\rangle-\langle\frac{\partial\tau_{sn}^{sgs}}{\partial n}\rangle$$

$s-n$: **Streamwise and wall-normal coordinates**

where $\overline{(..)}$ *is a filtered variable,* $\langle\cdots\rangle$ *is time-mean operator.*

- Integrate up to a matching location (Δ, U_Δ)

$$\langle\tau_w\rangle\approx-\left\langle\frac{\partial\overline{P}}{\partial s}\right\rangle\Delta-\int_0^\Delta[\langle\overline{u_s}\rangle\frac{\partial\langle\overline{u_s}\rangle}{\partial s}+\langle\overline{u_n}\rangle\frac{\partial\langle\overline{u_s}\rangle}{\partial n}]dn+\nu\frac{\partial\langle\overline{u_s}\rangle}{\partial n}\Big|_\Delta-\langle\overline{u_s}'\overline{u_n}'\rangle\Big|_\Delta-\langle\tau_{sn}^{sgs}\rangle\Big|_\Delta$$

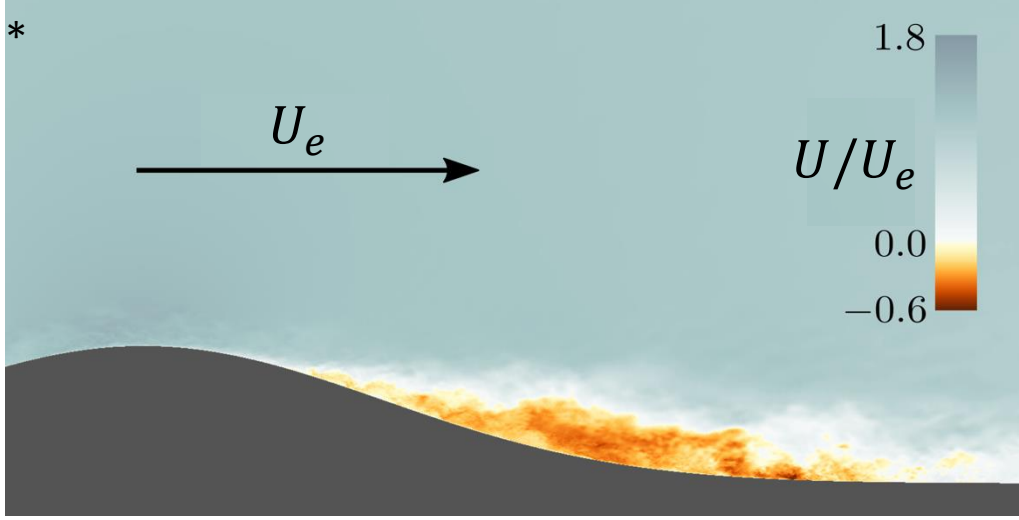
Total stress at outer LES matching location

- Near a separation point, two regions of the mean velocity profile are known
  - **Near wall – sqrt law (in pressure units)[1]**
  - **Overlap region – log law (in pressure units)[2]**

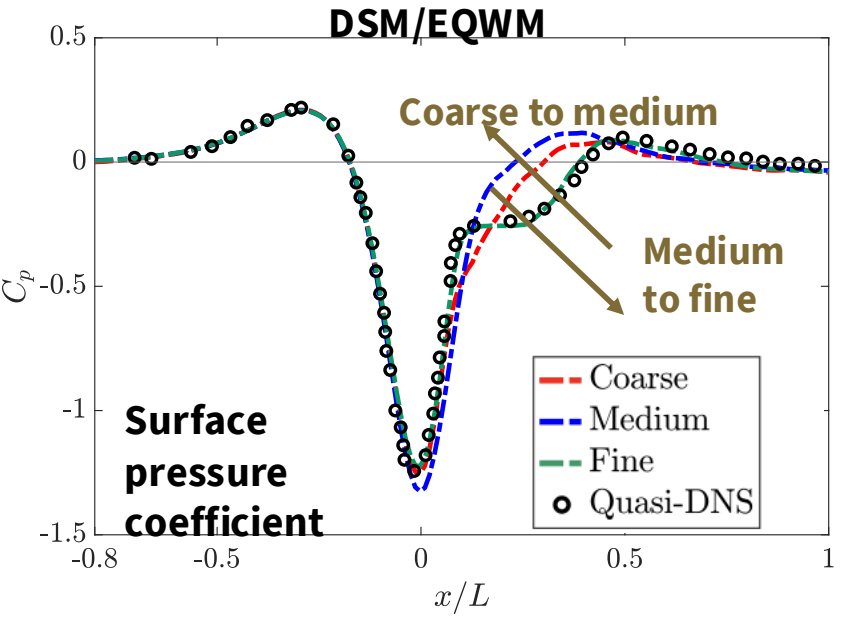
1: Stratford, JFM, 1959
2: Nickels, JFM, 2004

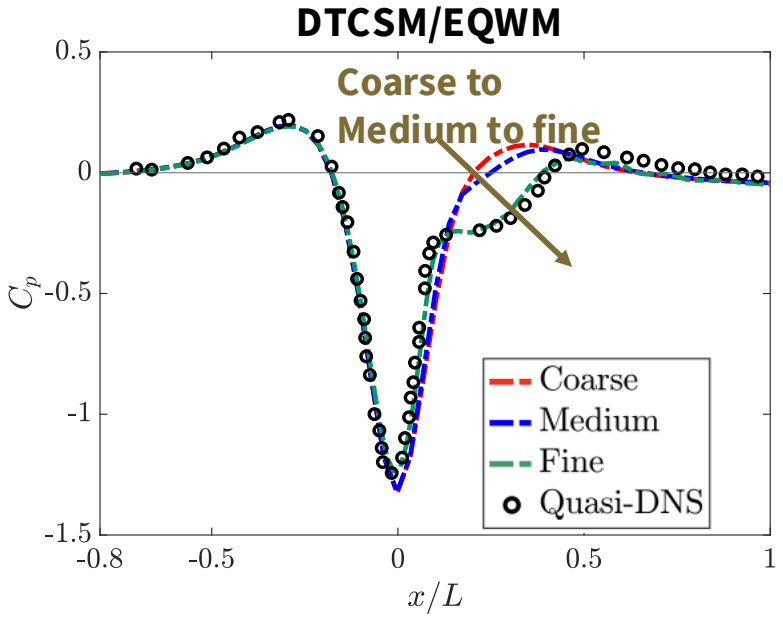
In this model, τ_w is linked to outer stress.
- We use DTCSM in this work

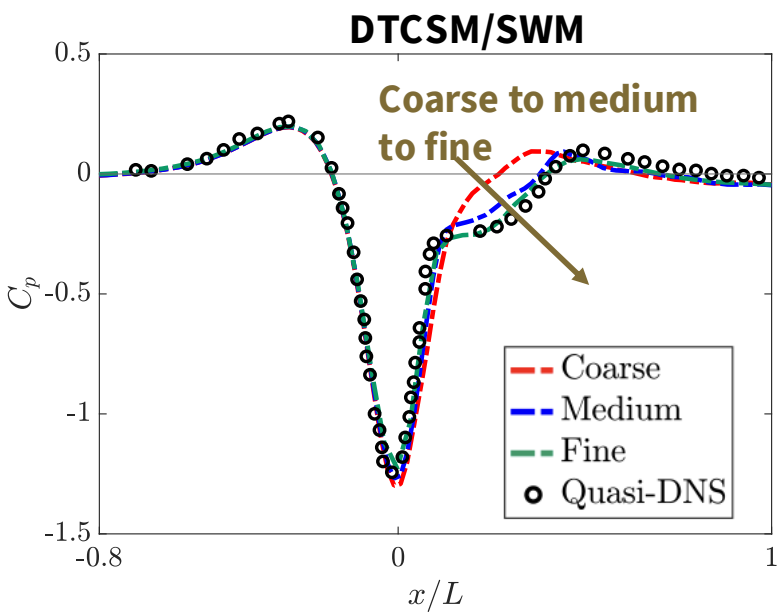
Validation Case I: Boeing speed bump



- Recall, DSM/EQWM produces a non-monotonically converging result
- DTCSM/EQWM provides monotonicity upon grid refinement but convergence is slow







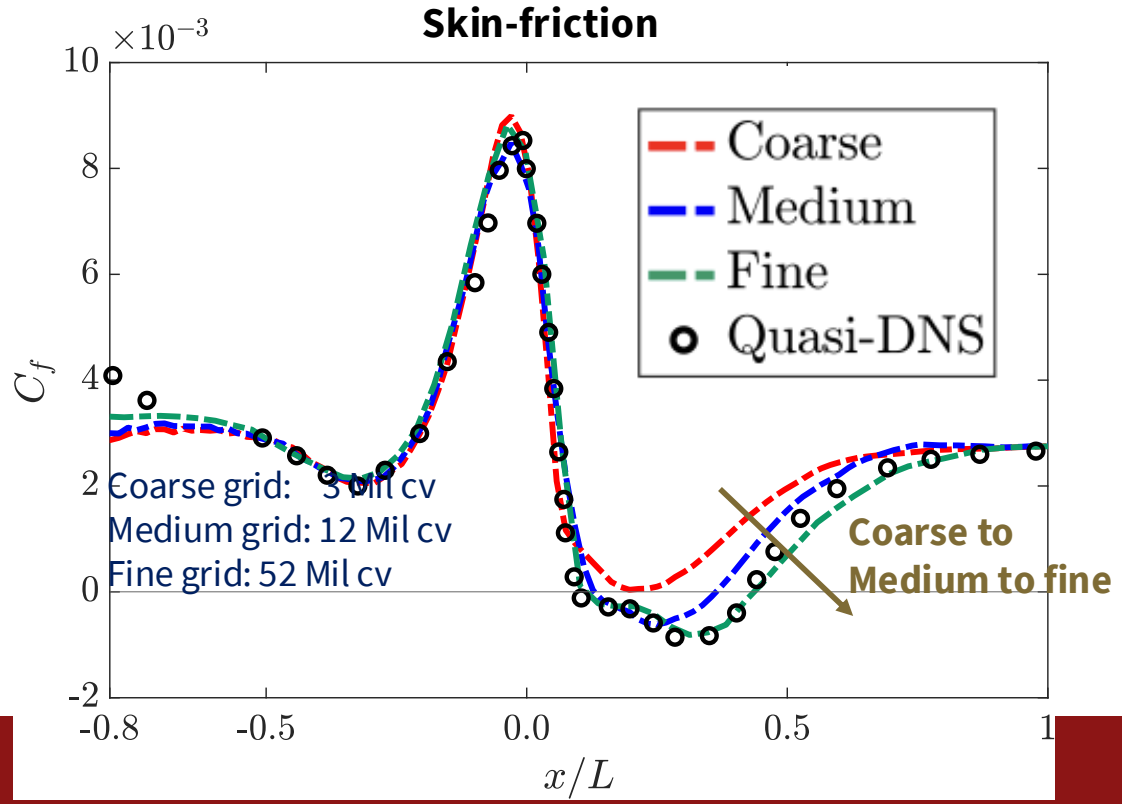
Coarse grid: 3 Mil CVs
Medium grid: 12 Mil CVs
Fine grid: 52 Mil CVs
Quasi-DNS: 10 Bcv

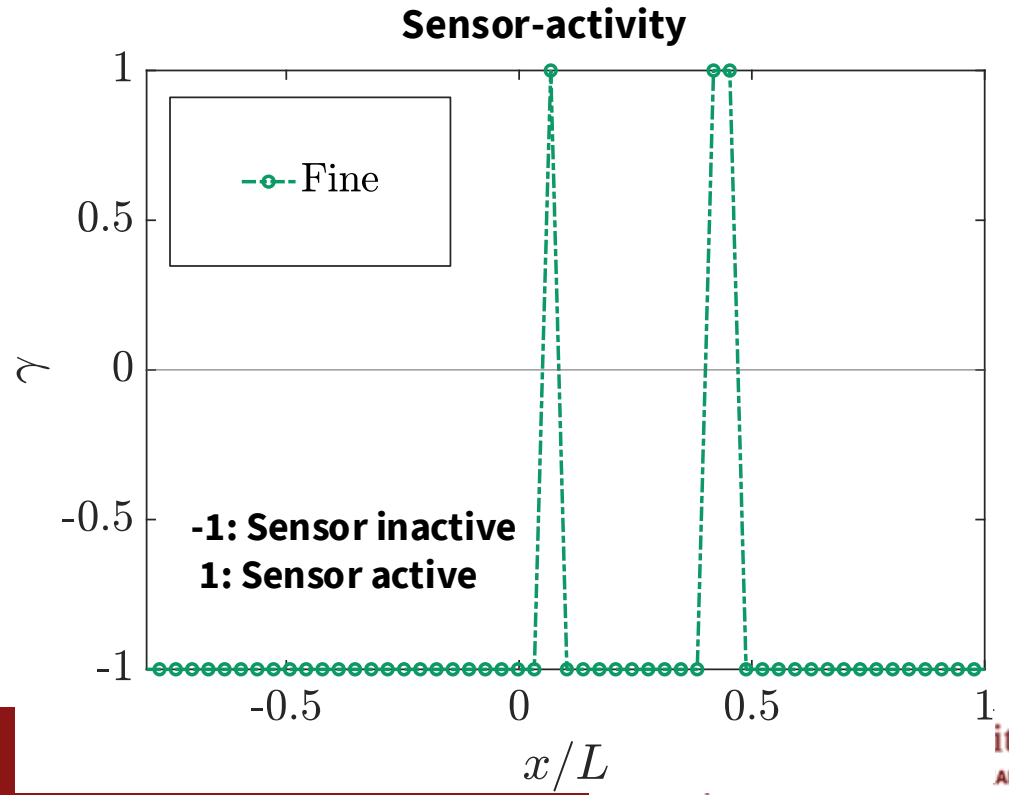
- **Sensor-based, non-eqbm. wall model provides improved accuracy on a 2x coarser grid (8x computational cost savings)**

Skin-friction prediction and activity of backflow sensor

- Skin-friction converges toward reference data monotonically
  - Agrees on fine grid, much improved predictions on medium grid.

- As the grid is refined, the extent of resolved non-equilibrium contribution increases
  - The backflow-sensor is expected to vary its activity based on resolved non-eqbm. content

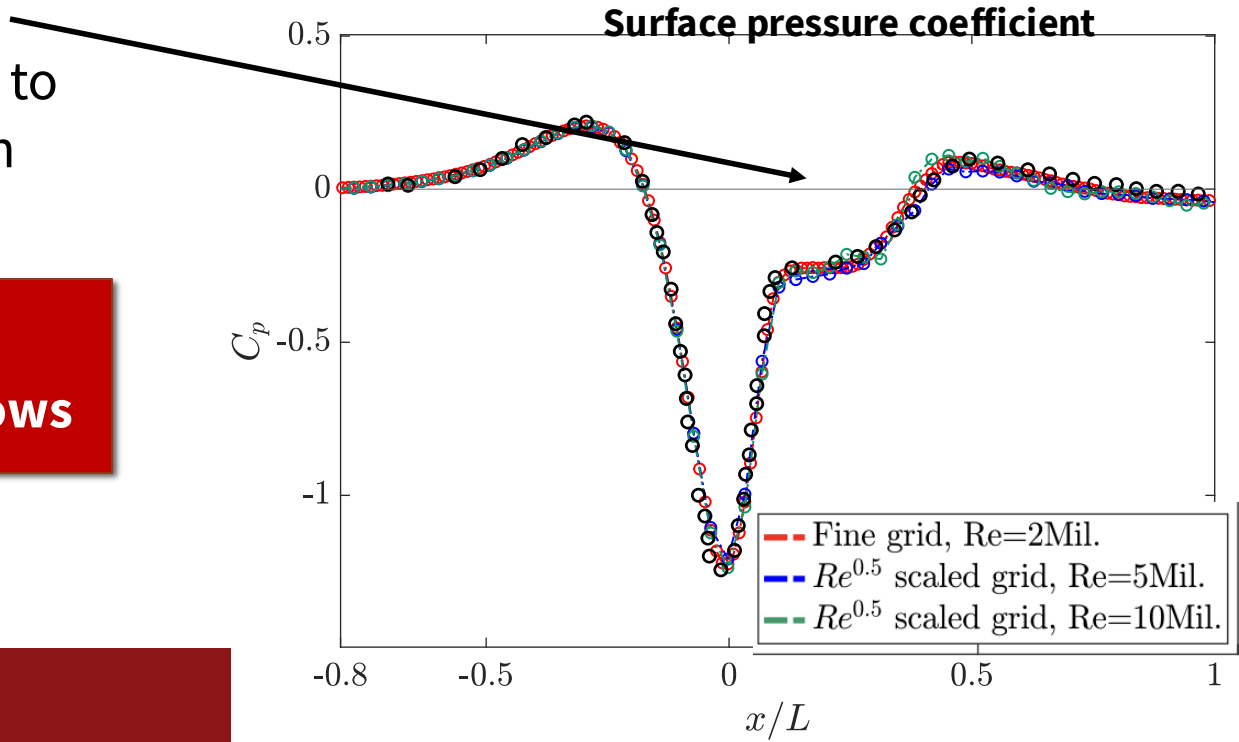




DTCSM/SWM converges at $N_{cv} \sim Re^1$ even for separated flows

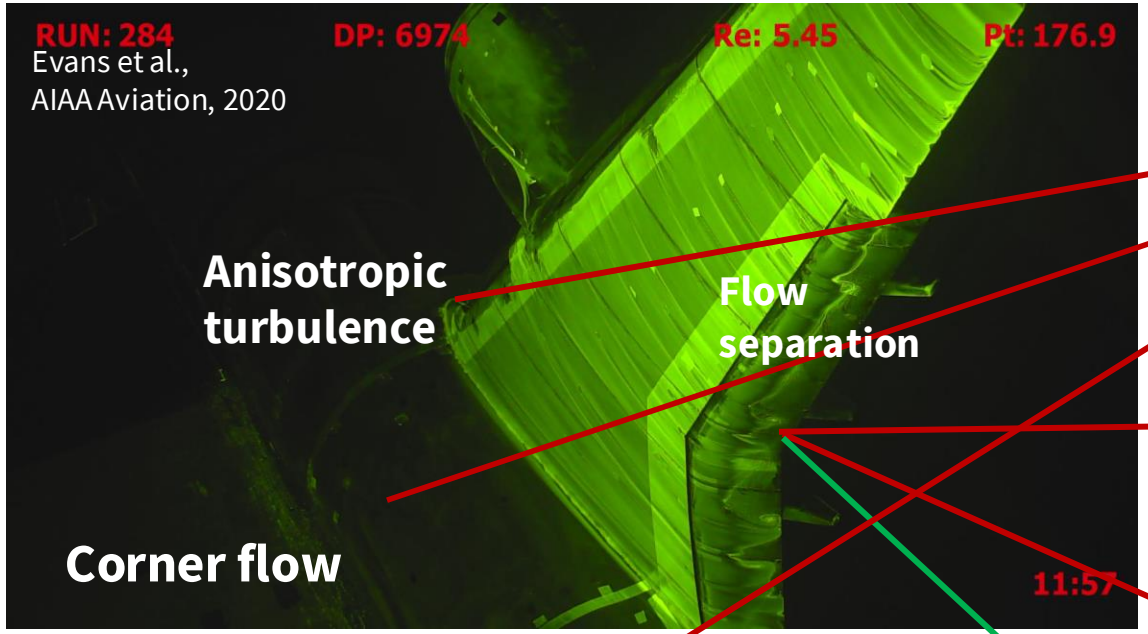
- An improved non-equilibrium wall-model is expected to have improved grid-point scaling (with Re) than EQWM ($N_{cv} \sim Re^{4/3}$)
- **Scaling arguments**:[1] wall-normally integrated non-eqbm terms near a sepn. point scale as $\Delta \times Re^{0.5} \times \frac{dC_p}{dx}$
  - *A-posteriori* WMLES using SWM converges to reference expts. for $\Delta \sim Re^{-0.5}$ resolution between $Re_L = [2 - 10] \times 10^6$

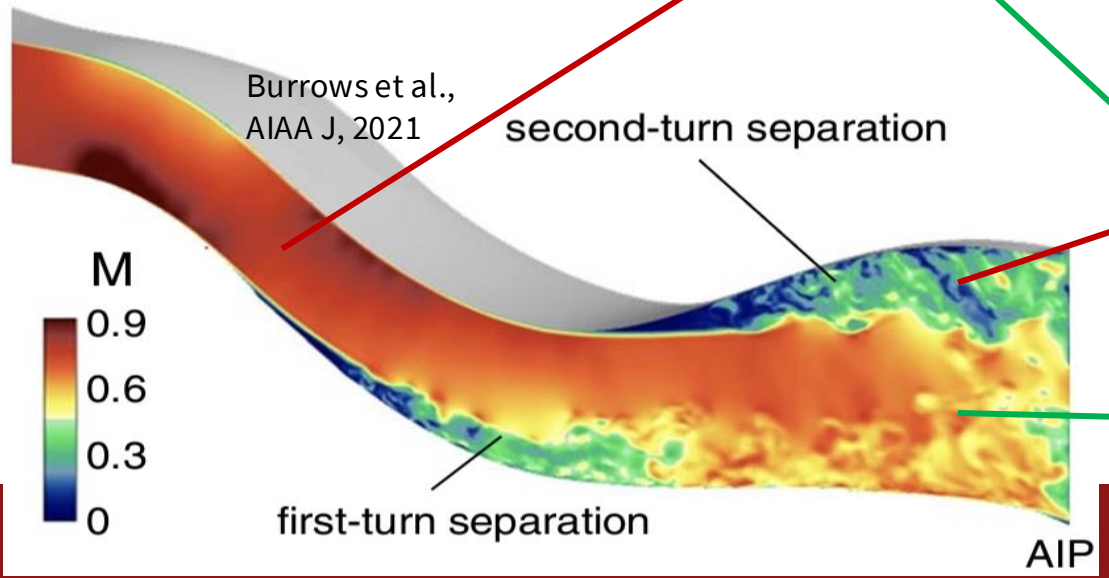
Proposed sensor-based wall model converges at $N_{cv} \sim Re^1$ for separated flows



1: Agrawal et al., under review, Phys. Rev. Fluids, 2024

Outline of this thesis





Alleviation of the Boussinesq hypothesis in SGS modeling

Grid point scaling of WMLES of separated boundary layers

Sensor based wall model for predicting smooth-body separation

WMLES of complex engineering flows underdoing separation

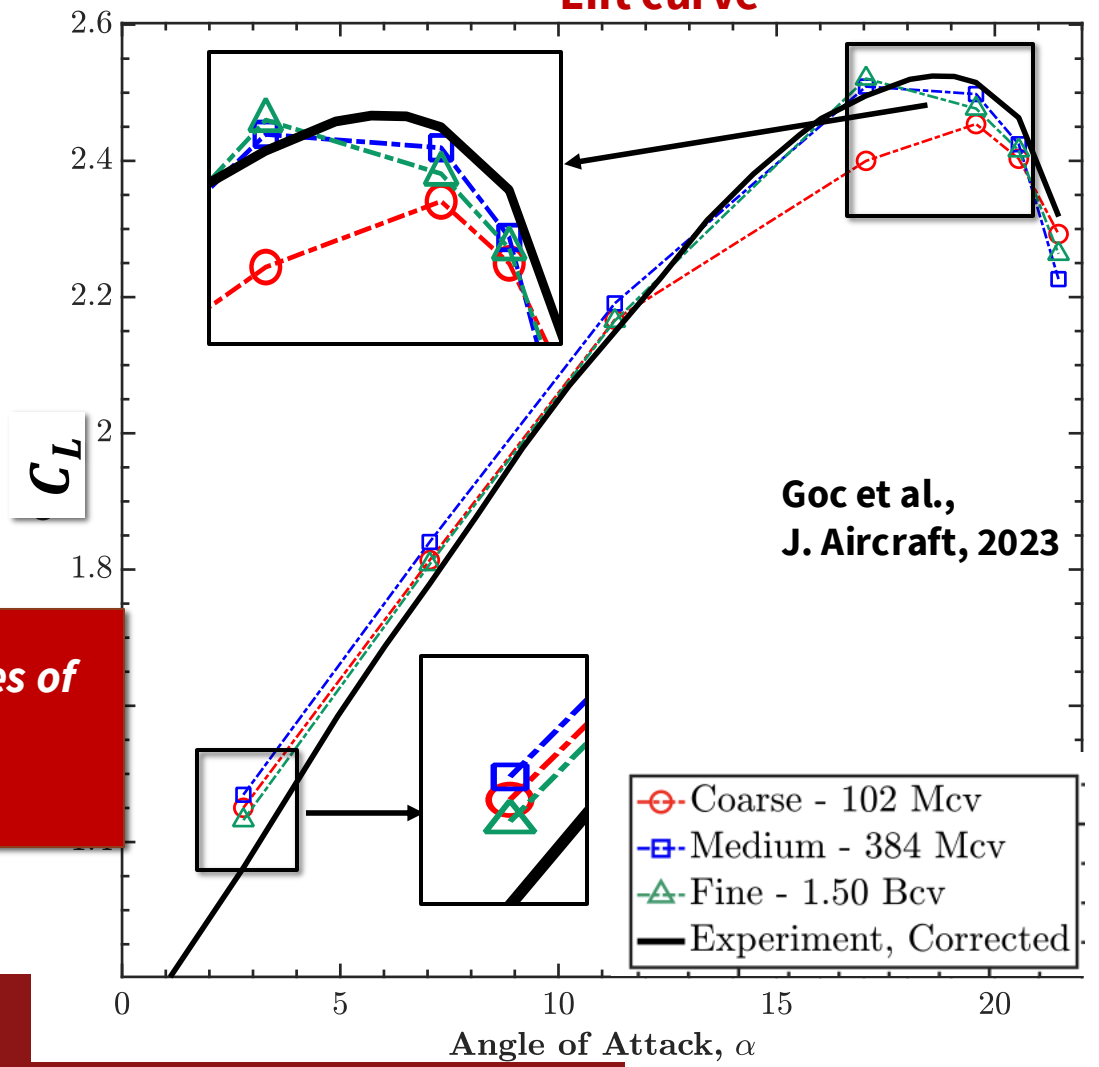
Application I: High Lift Common Research Model – QinetiQ

- **Test case in high-lift prediction workshop at AIAA SciTech, 2022**
- Half-span, free-air configuration
  - $\boldsymbol{Re_{MAC}} = \frac{U_e\,(MAC)}{\nu} = 5.49 \times 10^6,\ Ma = 0.2$
  - Wind-tunnel corrected data available



Goc et al.,
J. Aircraft, 2023

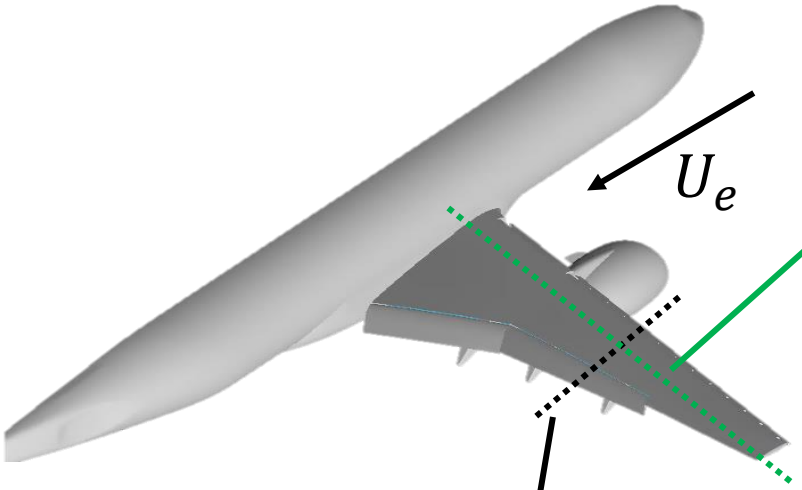
Lift curve

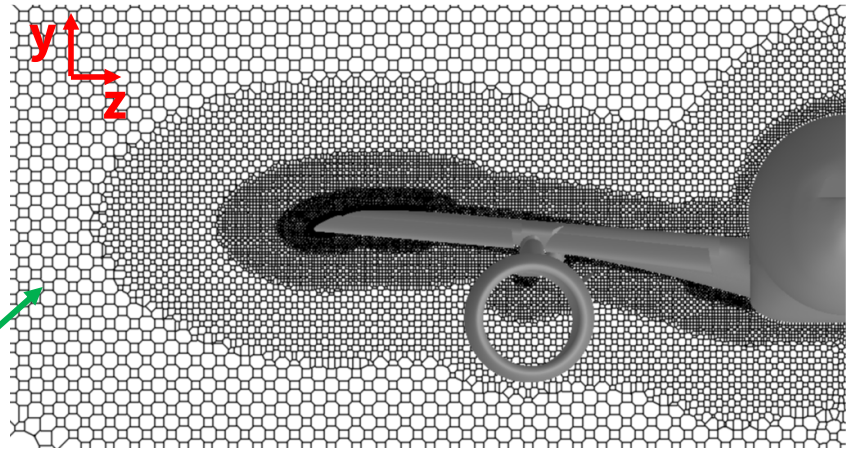


Workshop summary[1] : WMLES can predict maximum lift, but *at **low angles of attack**, predicting smooth body **separation over flaps** remains a **challenge** in both **accuracy and grid-to-grid monotonicity**.*

1: Kiris et al, *J. Aircraft*, 2023

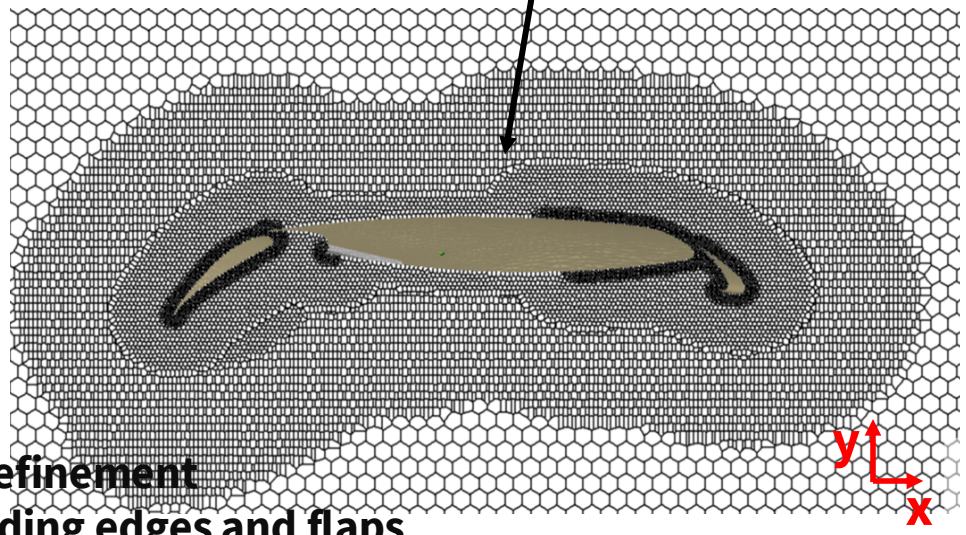
Gridding practice on CRM aircraft geometry



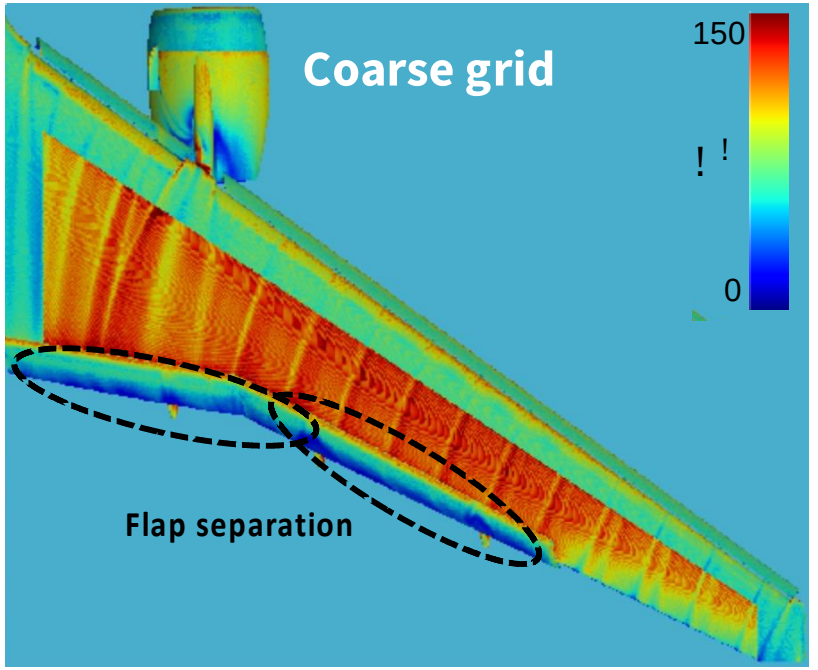


Darker region: refined grid

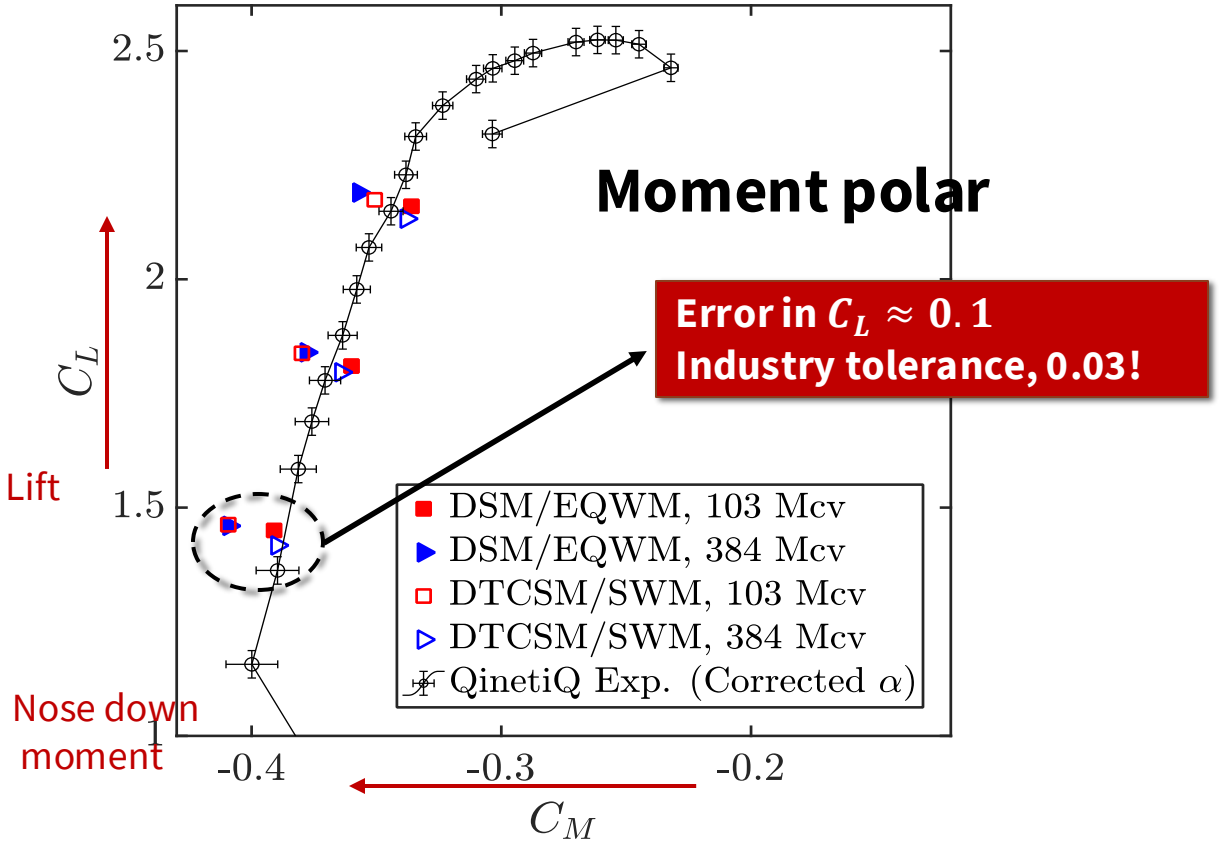
Targeted refinement around wing-tip, wing-root

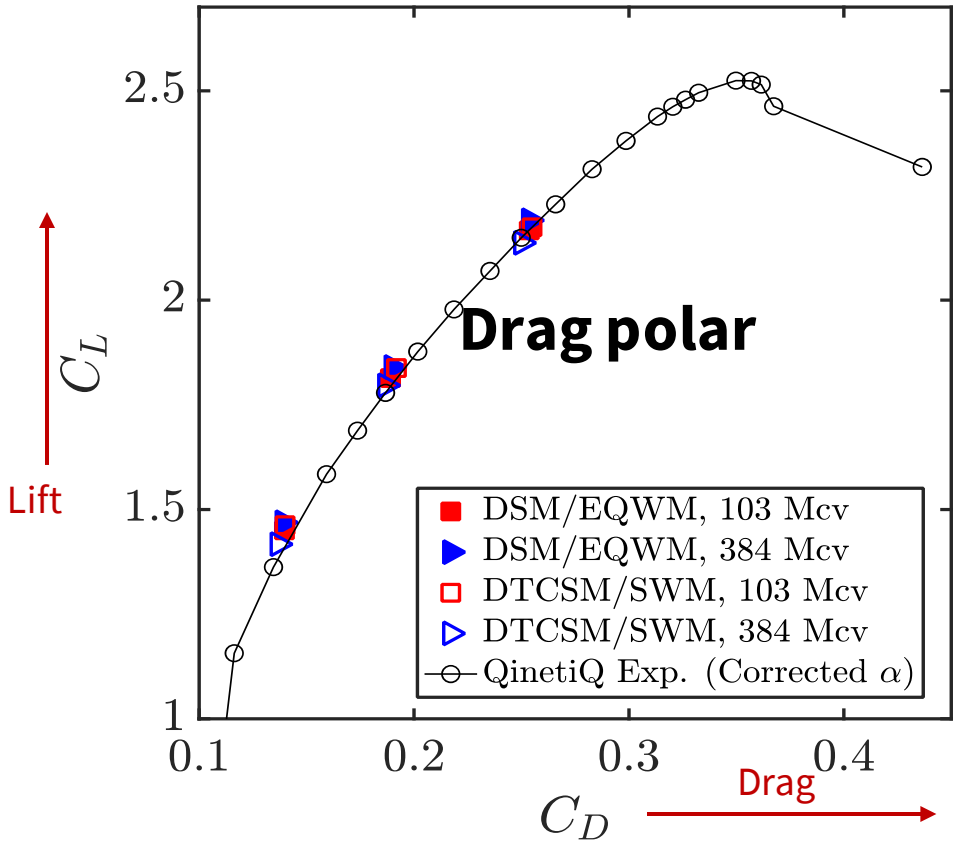


Targeted refinement around leading edges and flaps



DTCSM/SWM models predict lift, moment and drag accurately for low angles of attack, and on coarser grids than DSM/EQWM!

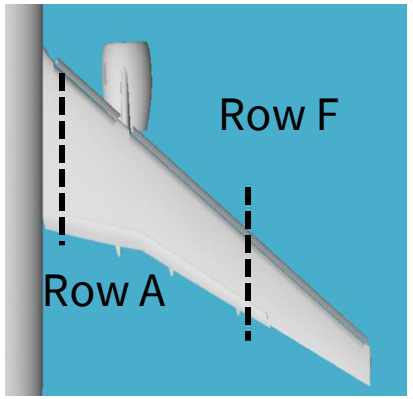


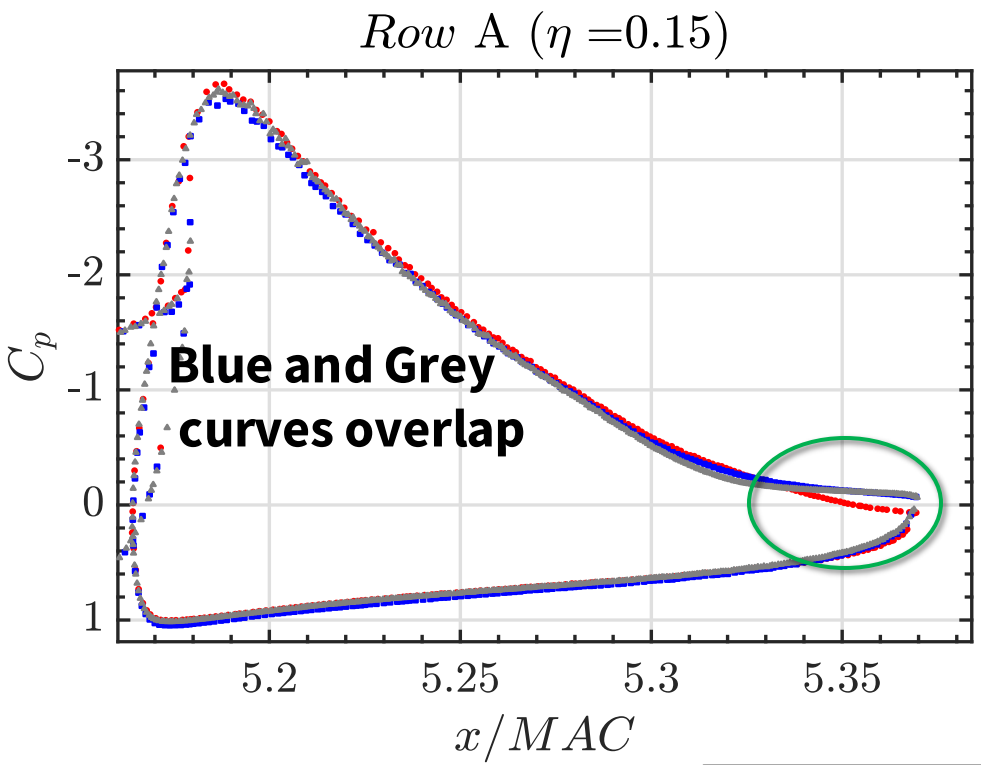


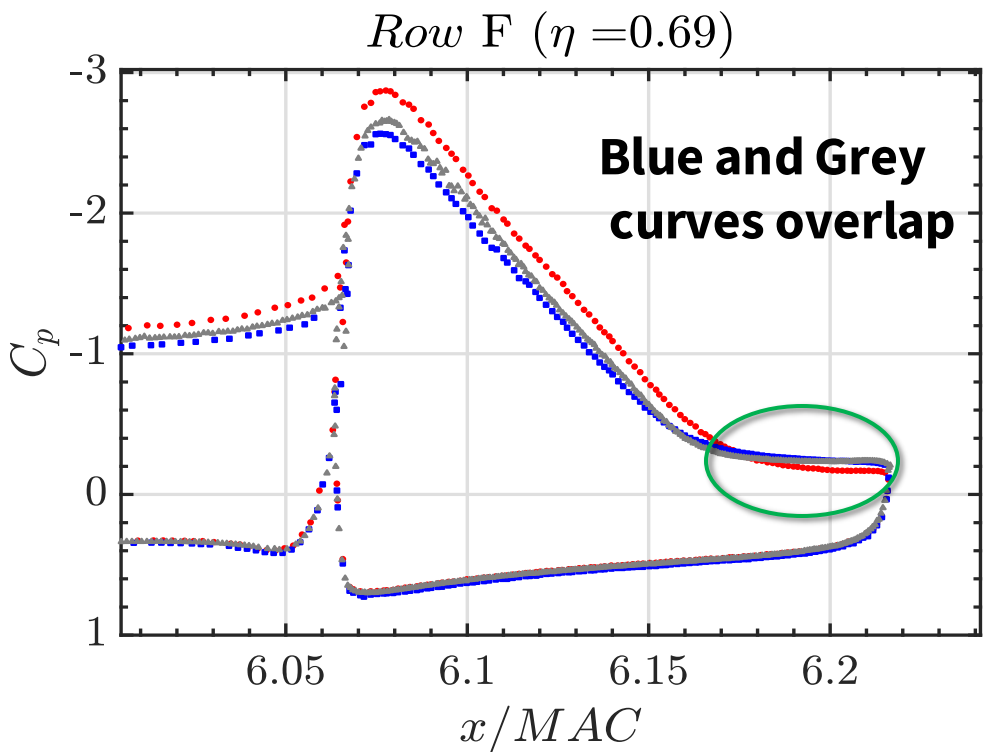
- **DSM/EQWM: Non-monotonic grid-dependence** of CL/CD, and CL/CM
  - Also reported in Goc et al., J. Aircraft 2023.
- **DTCSM/SWM models predict reasonable solution for 384 Mcv grid**
- DTCSM/EQWM monotonically converges, but requires at least 1500 Mcv grid (not shown)

Surface streamlines corroborate DSM/EQWM result in weaker flap separation

$[\alpha = 2.78^o]$



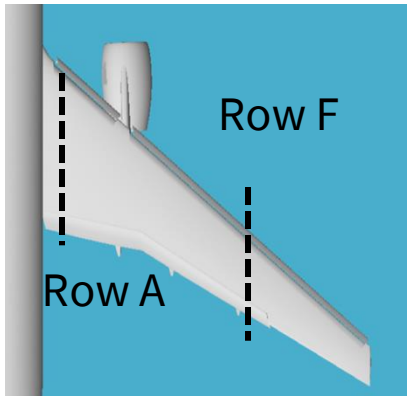


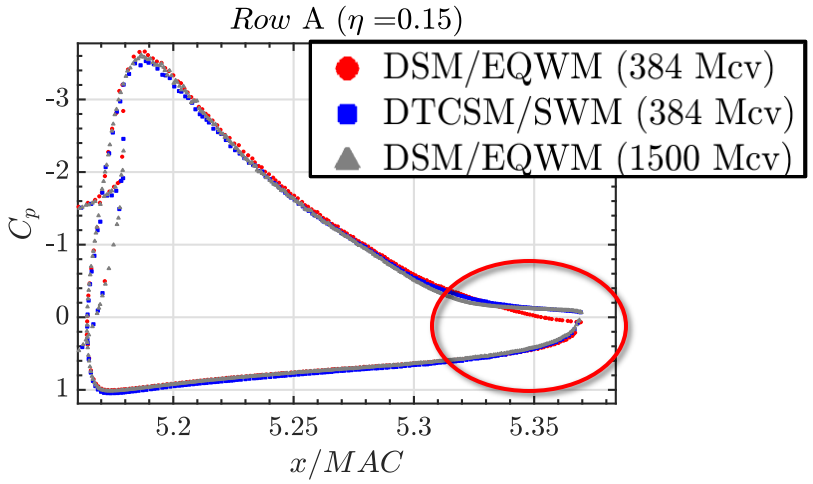


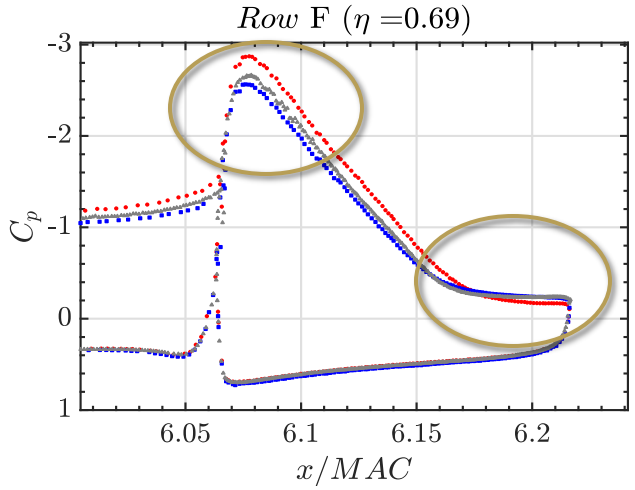
DSM/EQWM (384 Mcv)
DTCSM/SWM (384 Mcv)
DSM/EQWM (1500 Mcv)

Surface streamlines corroborate DSM/EQWM result in weaker flap separation

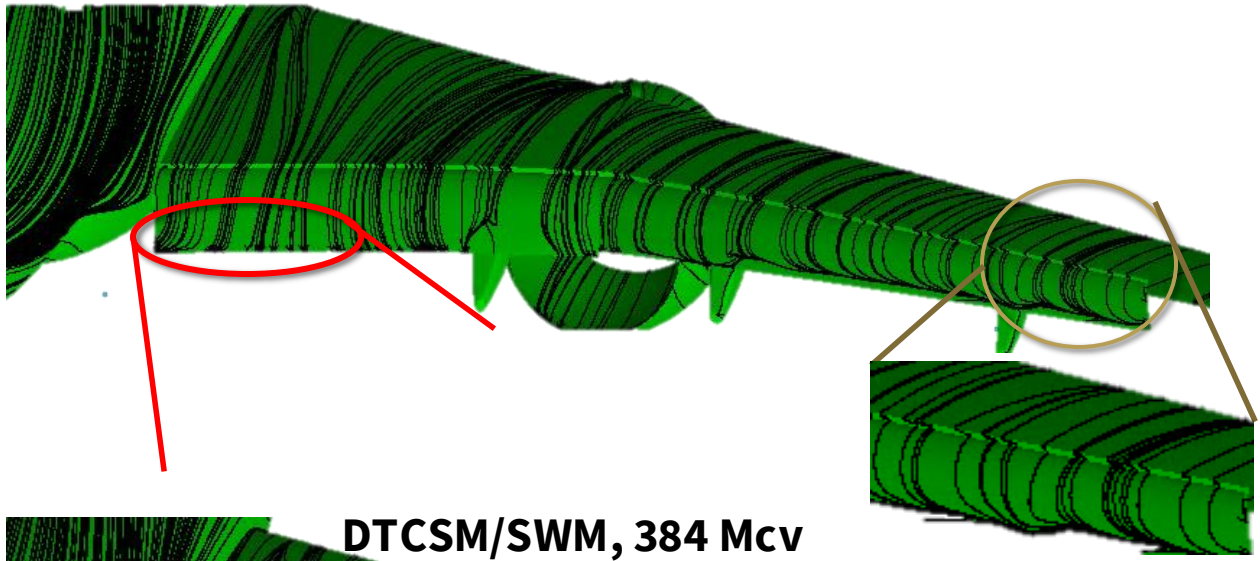
$[\alpha = 2.78^o]$



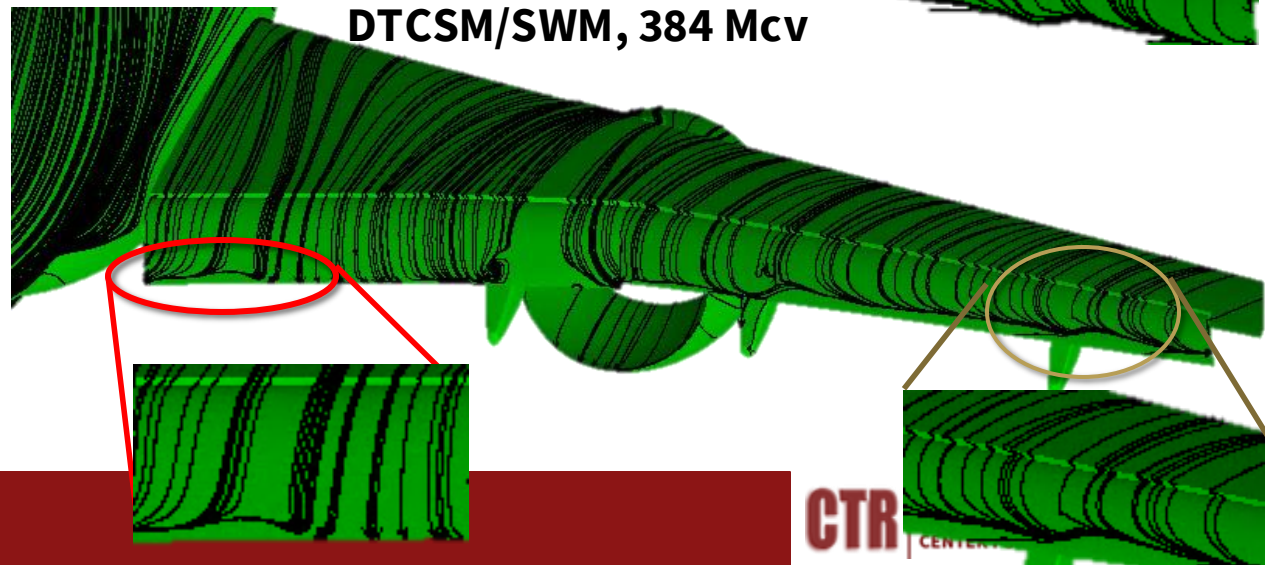




DSM/EQWM, 384 Mcv

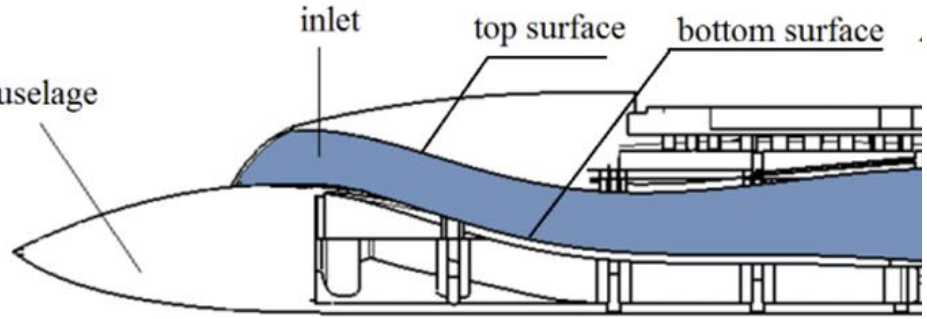


DTCSM/SWM, 384 Mcv

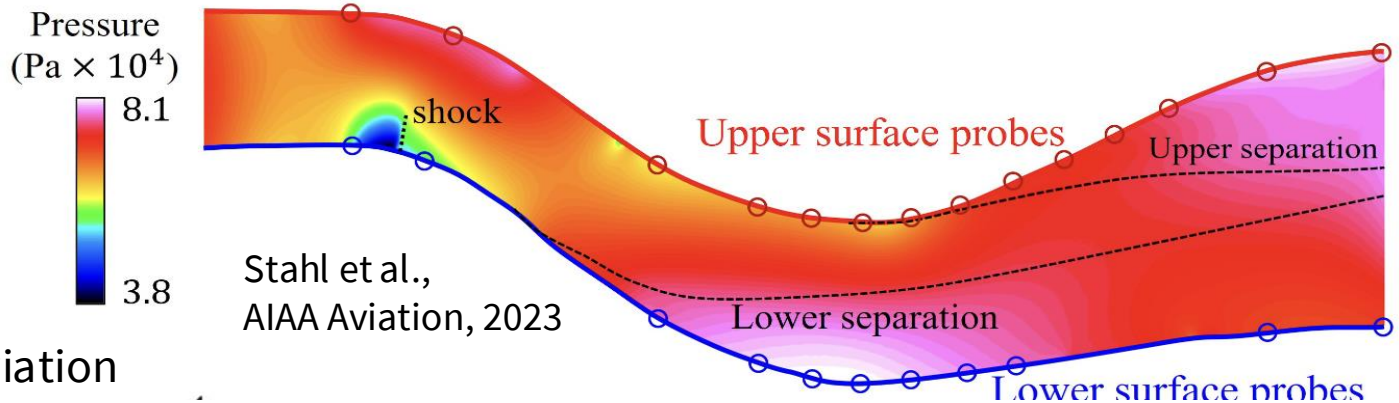


Application II: Transonic flow inside serpentine duct


From airsculptor.com website



Ge et al., IOP, 2020



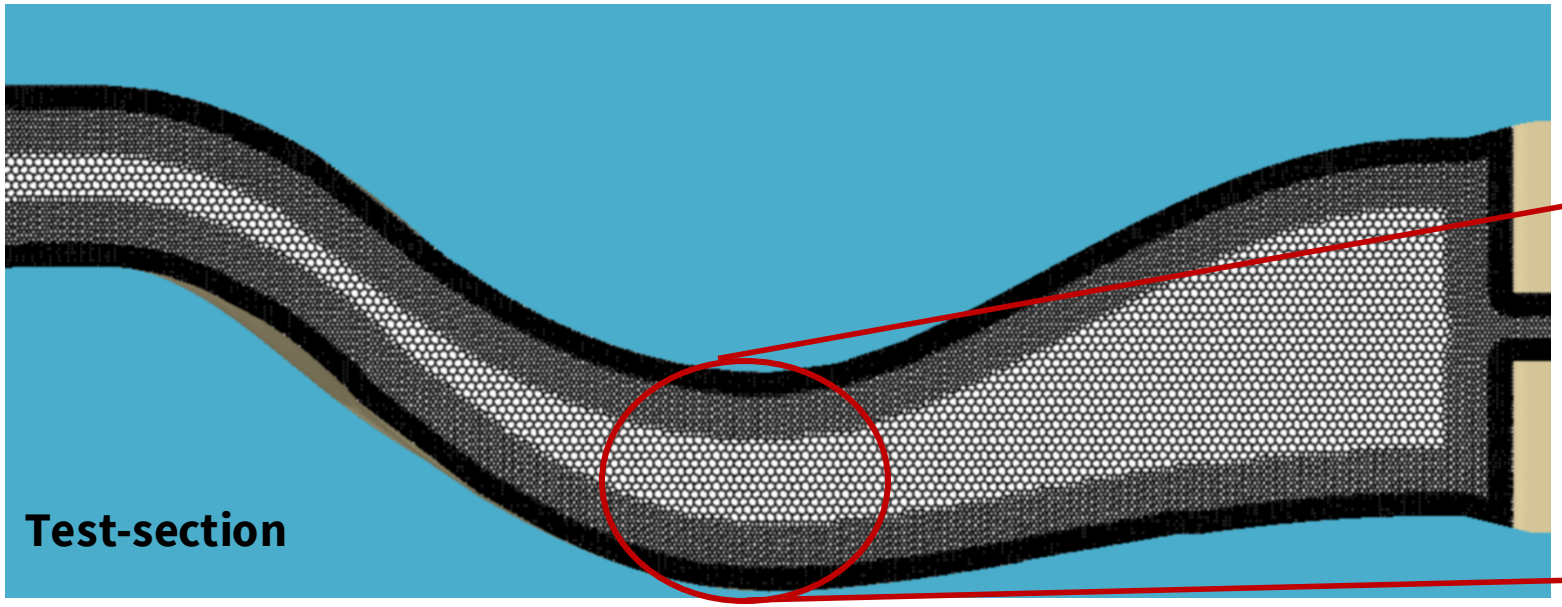
Stahl et al.,
AIAA Aviation, 2023

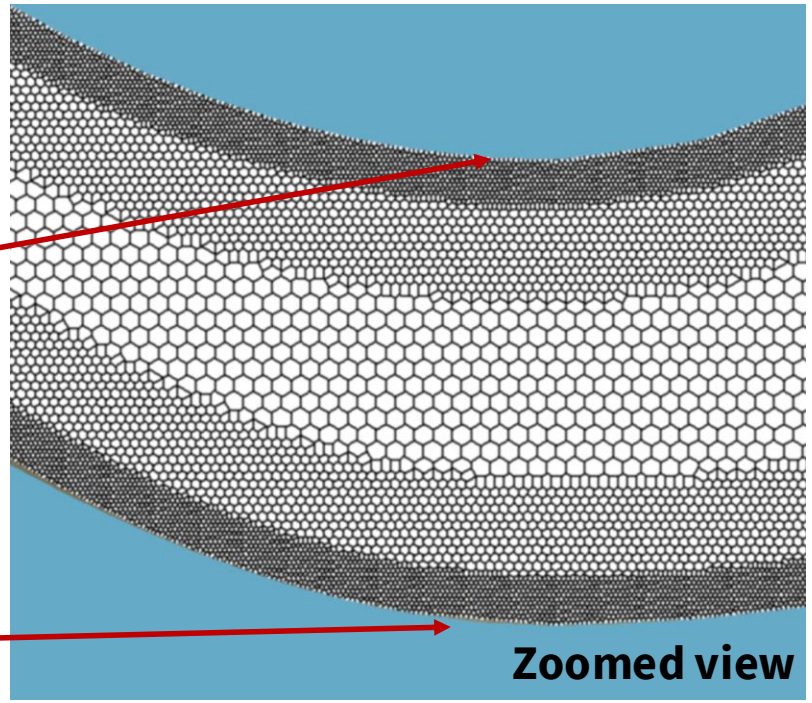
- Relevance: Propulsion applications, high-speed aviation
- **AIAA 2017 Propulsion Workshop summary[1]: *RANS, DES struggle to capture flow recovery at exit planes that result from complex, three-dimensional separations in the duct***

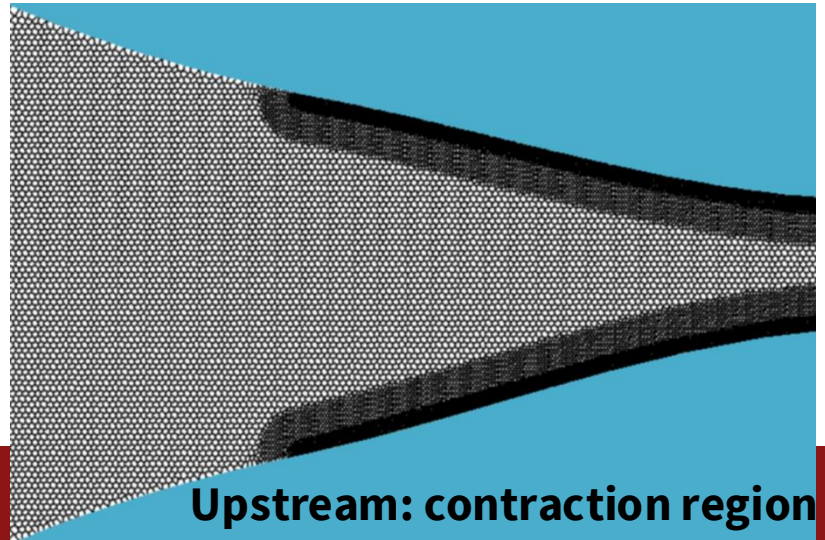
1. Winkler and Davis, AIAA, 2017

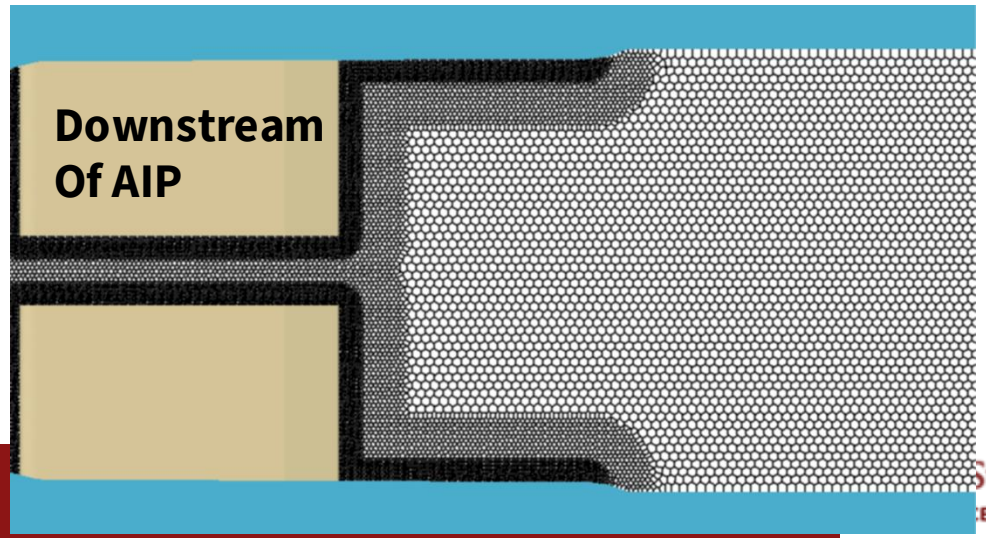
Quantity of interest: Flow recovery at exit

Schematic of grid topology

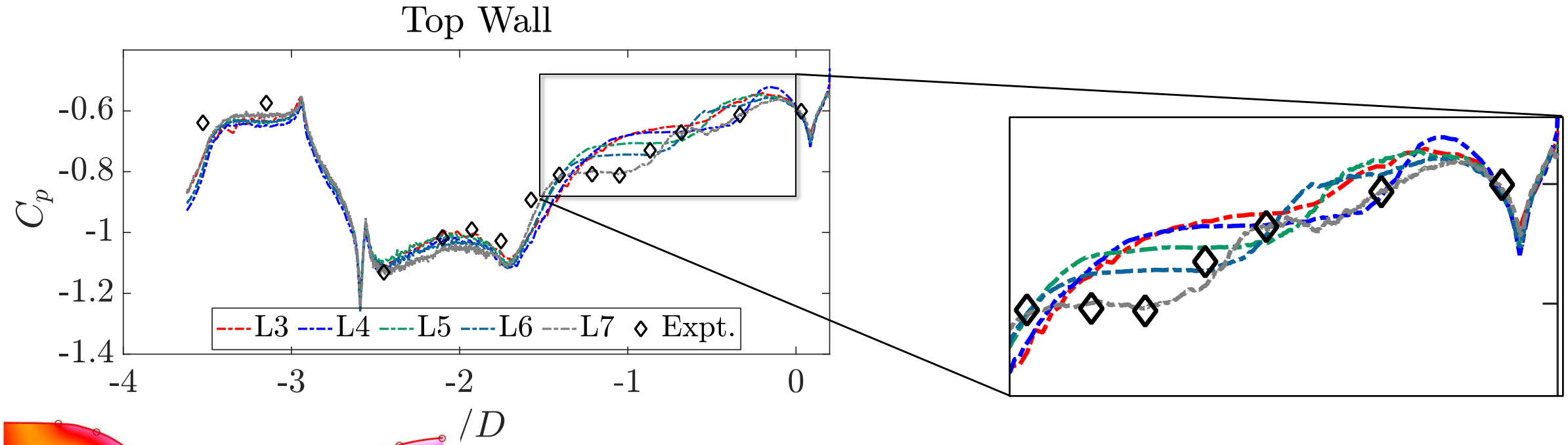


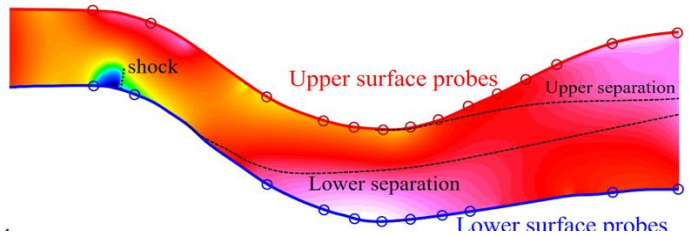






DTCSM/SWM: Grid refinement sequence for top-wall surface pressure

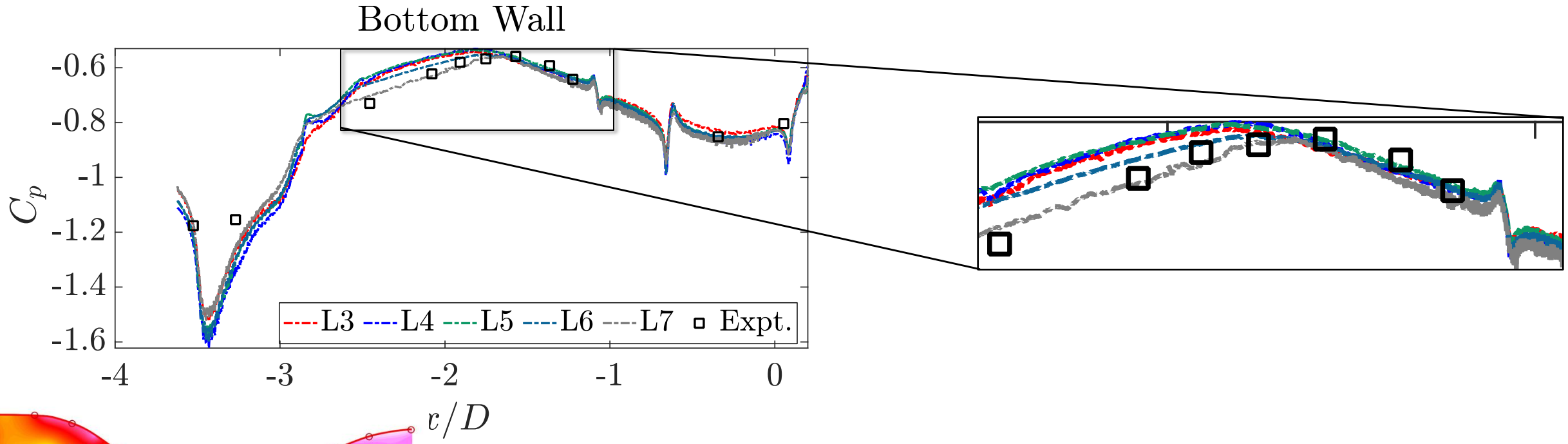


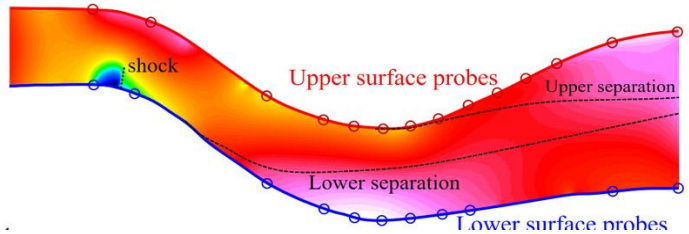


L3: 31 Mcv
L4: 89 Mcv
L5: 350 Mcv
L6: 1500 Mcv
L7: 3000 Mcv

- DTCSM/SWM approaches the expt. monotonically with grid-refinement
- **L7 grid agrees reasonably with experiments**

DTCSM/SWM: Grid refinement sequence for bottom wall surface pressure

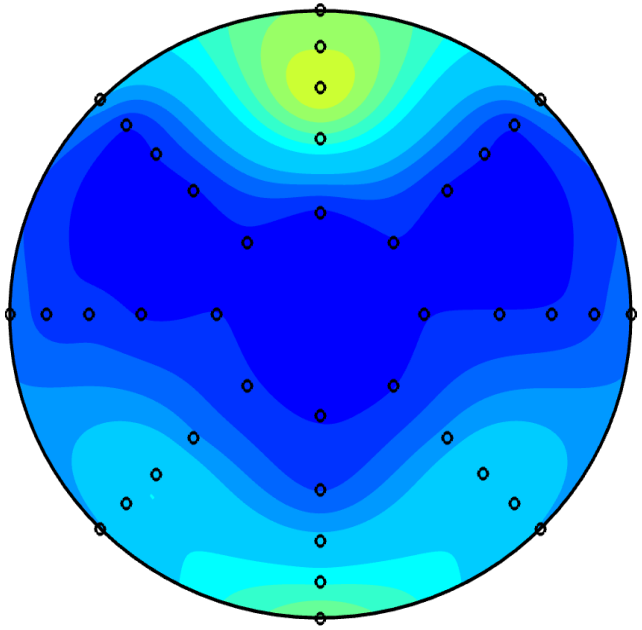


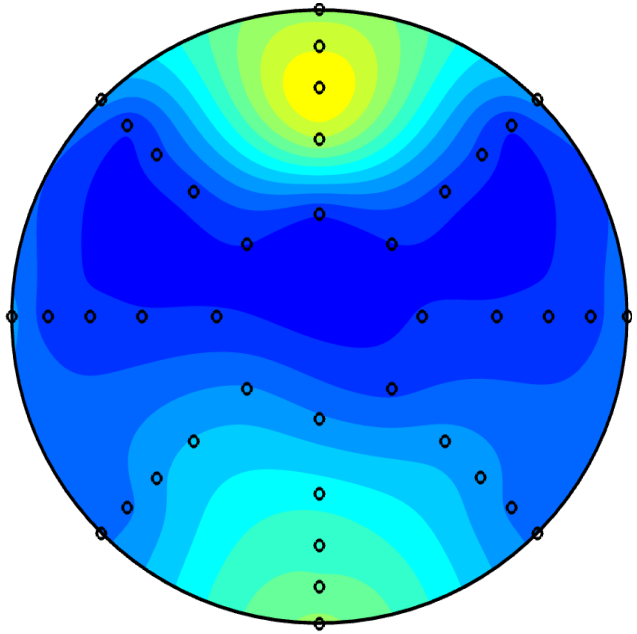


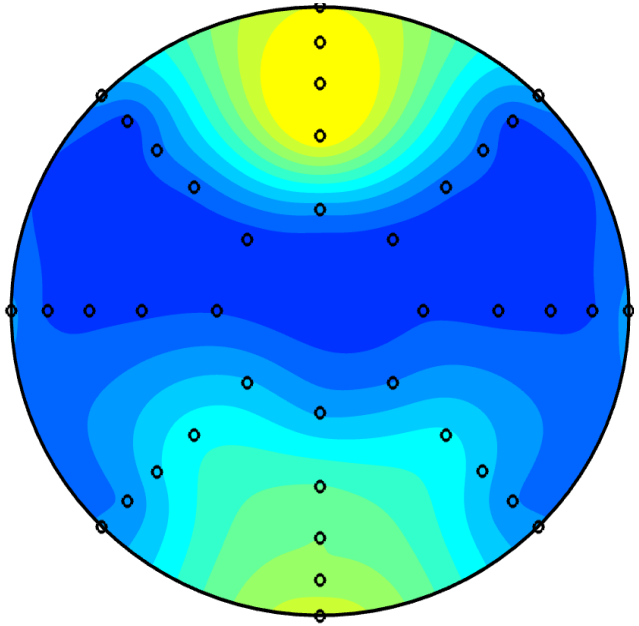
L3: 31 Mcv
L4: 89 Mcv
L5: 350 Mcv
L6: 1500 Mcv
L7: 3000 Mcv

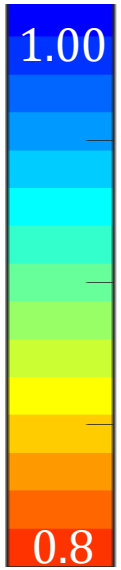
- DTCSM/SWM approaches the expt. monotonically with grid-refinement
  - **Unlike DSM/EQWM (not shown)**
- **L7 grid agrees reasonably with experiments**
  - DSM/EQWM underpredicts separation on all grids (not shown)

DTCSM/SWM: Grid dependence of mean flow recovery at AIP

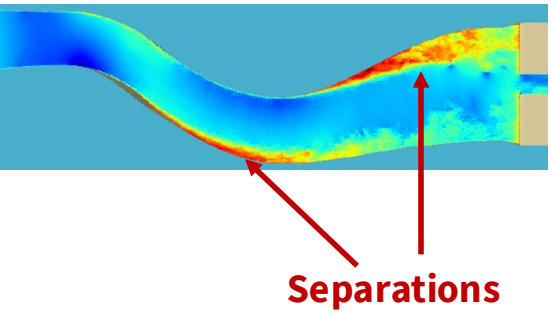








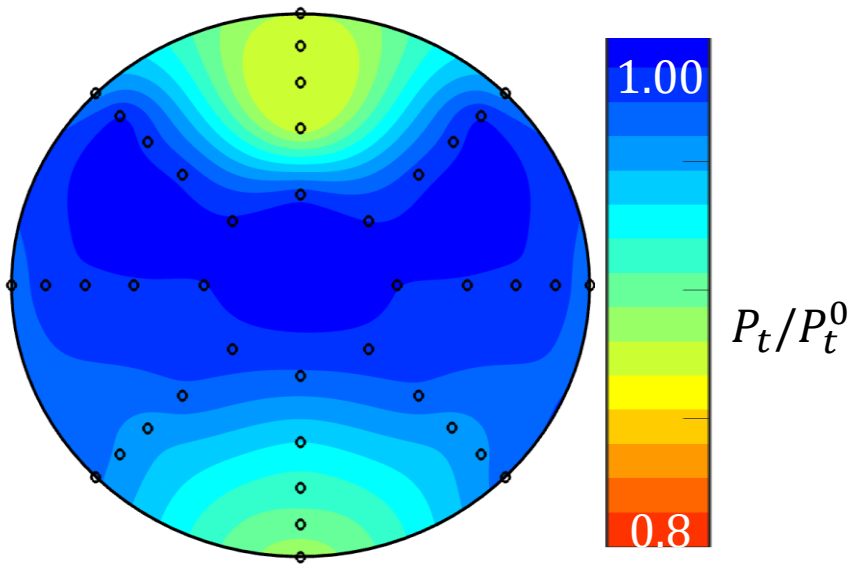
L5 grid, PR: 0.961 ± 0.01 (rms) **L6 grid, PR: 0.957 ± 0.01** **L7 grid, PR: 0.951 ± 0.01**



- **On both walls, the pressure loss at "midspan" increases with grid-refinement**
  - Increasing separation intensity on top wall leads to higher loss in dynamic pressure
  - Onset of separation on bottom wall leads to more losses on bottom wall
- Lowered net pressure recovery as the grid is refined $\left(\mathbf{PR} = \frac{1}{N^{dyn.rakes}} \frac{\sum^{N^{dyn.rakes}} P_t^{AIP}}{P_{inlet}}\right)$

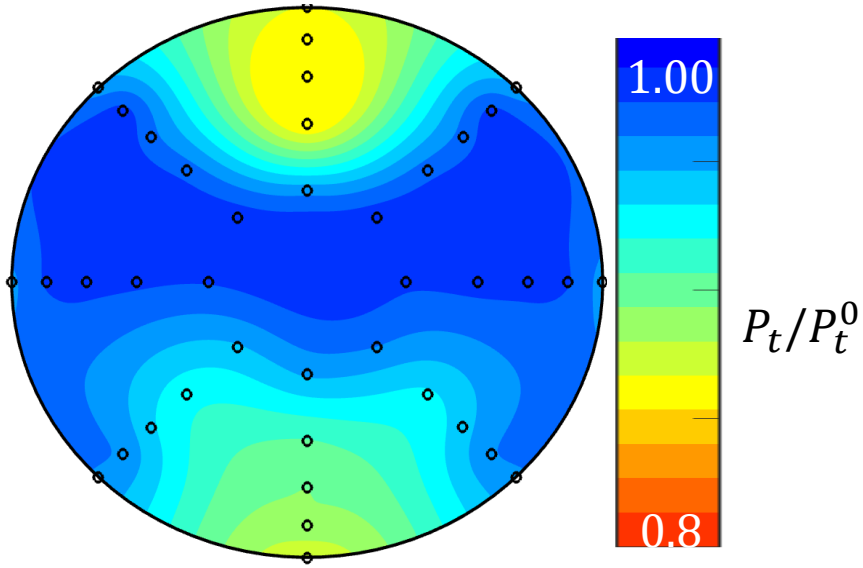
DSM/EQWM vs DTCSM/SWM: Mean pressure recovery

L7, DSM/EQWM



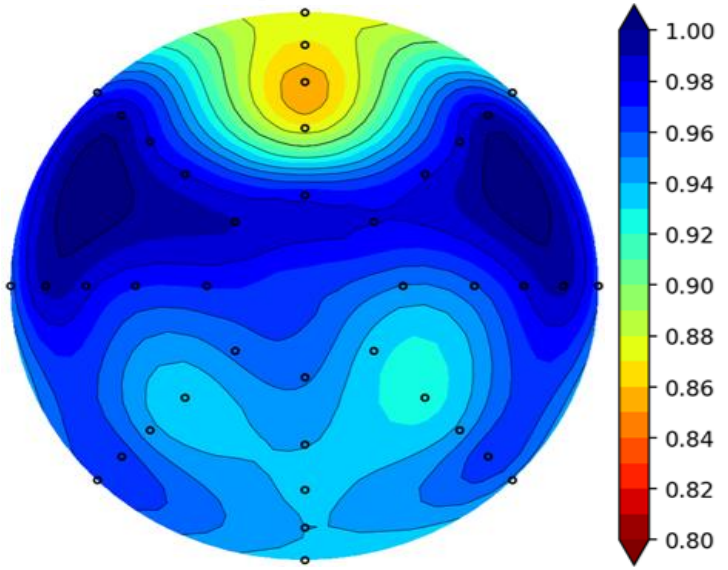
PR: 0.961 ± 0.01 (rms)

L7, DTCSM/SWM



PR: 0.951 ± 0.01 (rms)

Experiment



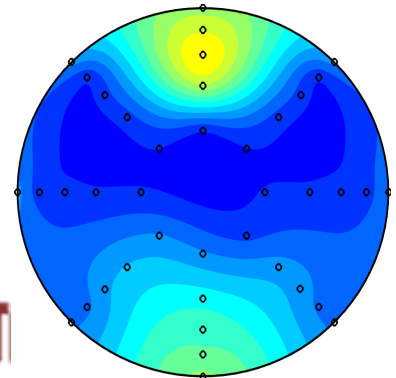
PR: 0.953 ± 0.01
(uncertainty per Burrows et al., 2020)

Previous recovery results: Lakebrink et al. , AIAA Aviation, 2019: DES: 0.959

- **DTCSM/SWM qualitative agrees more with expt. (larger bottom separation)**
- DSM/ SM/SWM!

DTCSM/SWM outperforms DSM/EQWM in predictions of separations and flow recovery at exit of the SD-2 serpentine duct!

L6, DTCSM/SWM



Concluding remarks

- **Dynamic, non-Boussinesq subgrid-scale model[1]**
  - Alleviates the classical misalignment problem between subgrid-stresses and strain-rates
  - Validated and verified in isotropic turbulence, channel flow
  - Boeing speed bump: Smooth body separation predicted, rectified issue of nonmonotonic grid convergence

- **Grid-point requirements for equilibrium assumptions based WMLES of separated flows[2]**
  - $N_{cv} \sim Re^{4/3}$: more expensive than classical $N_{cv} \sim Re^{1}$ scaling for attached equilibrium flows

- **Localized backflow sensor[3,4] to identify imminent flow separation and augment τ_w**
  - Boeing speed bump: Demonstrated improved accuracy than EQWM
  - Recovers $N_{cv} \sim Re^{1}$ even for separated flows

- **Applications in complex engineering flows**
  - Smooth body sep^{n} on flaps of High-Lift CRM: Improved accuracy and grid-convergence properties
  - Mean flow recovery prediction at the outlet of a serpentine duct

Obtained solutions within industry tolerance bounds.
Wall clock times $<$ 1 day using 3-4% Frontier nodes.

1: Agrawal et al., Phys. Rev. Fluids, 2022
2: Agrawal et al., AIAA J, 2024
3: Agrawal et al., Phys. Rev. Fluids, 2024
4: Agrawal et al., Flow, 2024

List of relevant publications

Non-Boussinesq SGS model

1. Agrawal et al., "Non-Boussinesq subgrid-scale model with dynamic tensorial coefficients," *Phys. Rev. Fluids,* 2022

***Re* dependence of grid points for WMLES of separated flows**

1. Agrawal, Bose, and Moin, "Reynolds number scaling of grid point requirements for wall-modeled LES of separated flows," *AIAA Journal*, 2024

Modeling of non-equilibrium turbulent boundary layers

1. Agrawal, Bose, and Moin. "Non-equilibrium wall model for predicting smooth body separation", *Phys. Rev. Fluids,* 2024
2. Agrawal et al., "An extension of Thwaites' method for turbulent boundary layers," *Flow,* 2024
3. Agrawal, Elnahhas, and Moin, Wall modeled large-eddy simulations of flow over Sandia transonic hump, *AIAA Aviation*, 2023

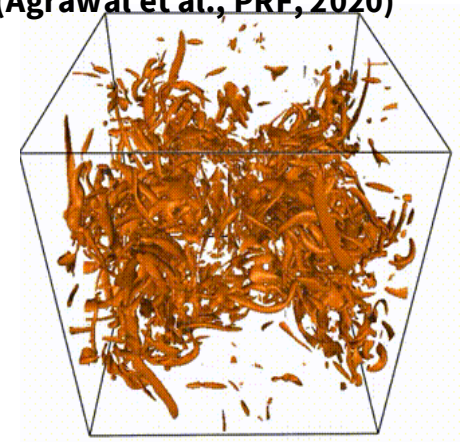
Prediction of loads in Common Research Aircraft models

1. Goc, Agrawal et al., "Large Eddy Simulation of the Transonic NASA Common Research Model," *J. Aircraft,* 2024
2. Agrawal et al., "Wall-modeled LES of high-lift common research model aircraft up to flight Reynolds number in the NTF wind-tunnel," *in prep for J. Aircraft*
3. Agrawal et al., "Reynolds number sensitivities in wall-modeled large-eddy simulations of a high-lift aircraft," *AIAA Aviation,* 2024
4. Agrawal, Bose, and Moin, "A non-equilibrium wall model: application to linear regime of a high-lift aircraft model," *AIAA SciTech*, 2025

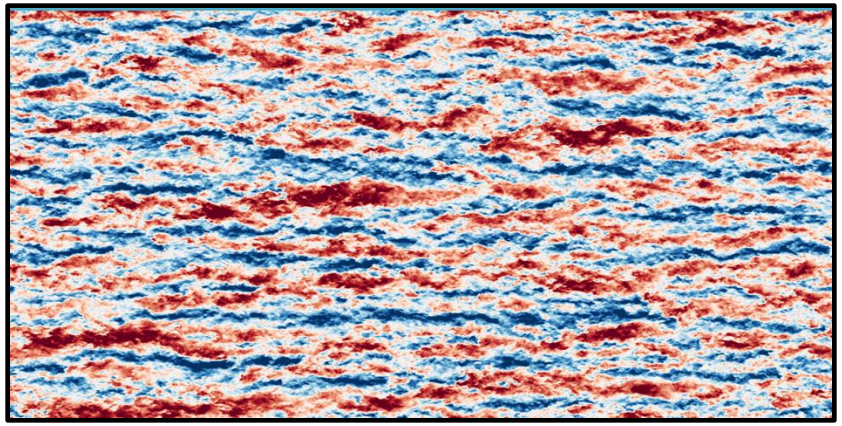
Flow distortions inside SD-2 diffuser

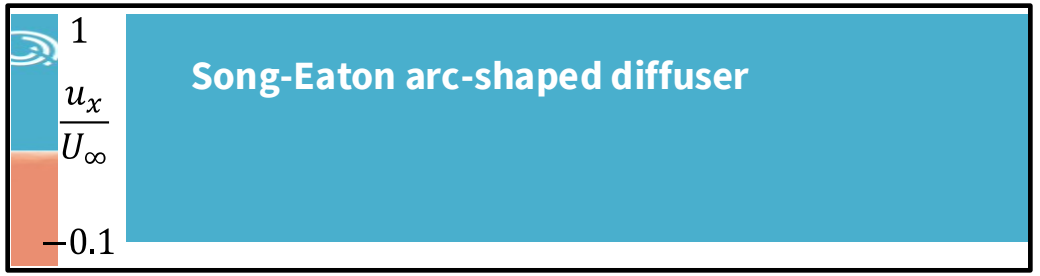
1. Agrawal, Bose, and Moin, "Prediction of flow distortions inside a serpentine diffuser from wall-modeled LES," *to appear, AIAA Aviation,* 2025

Homogeneous Turbulence
(Agrawal et al., PRF, 2020)



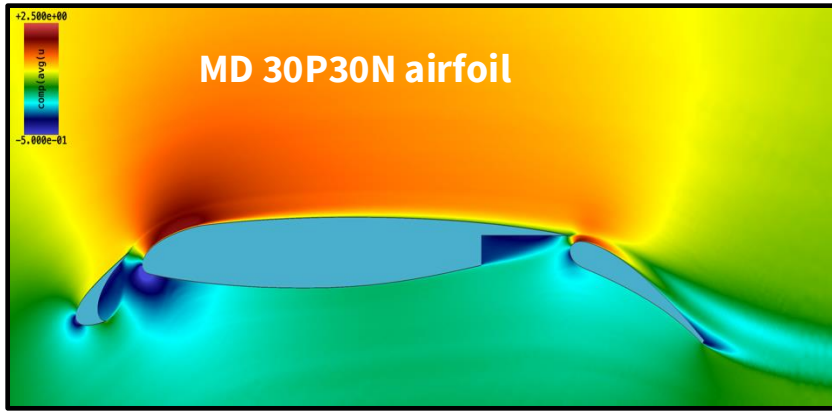
Channel flow

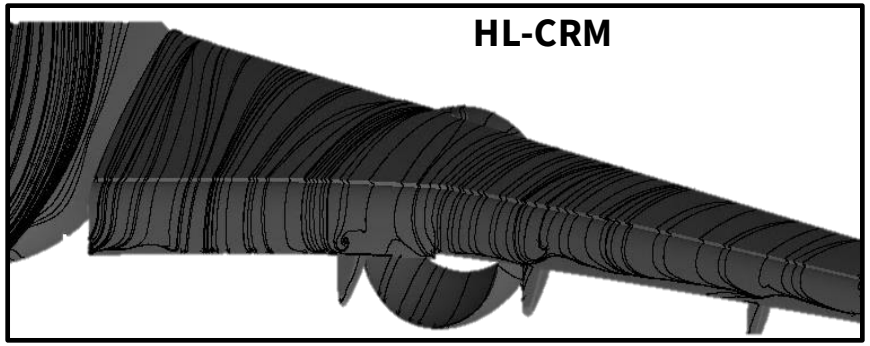


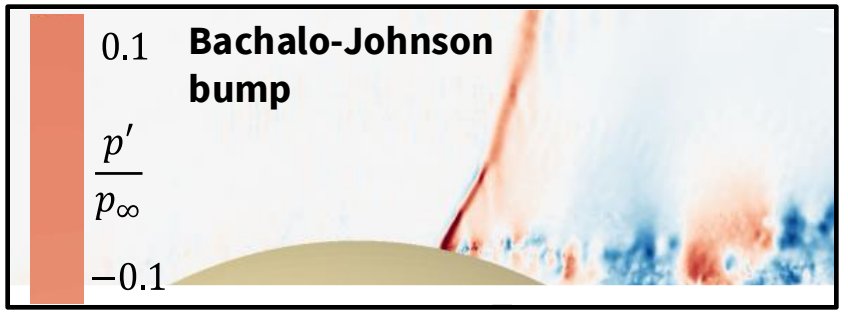


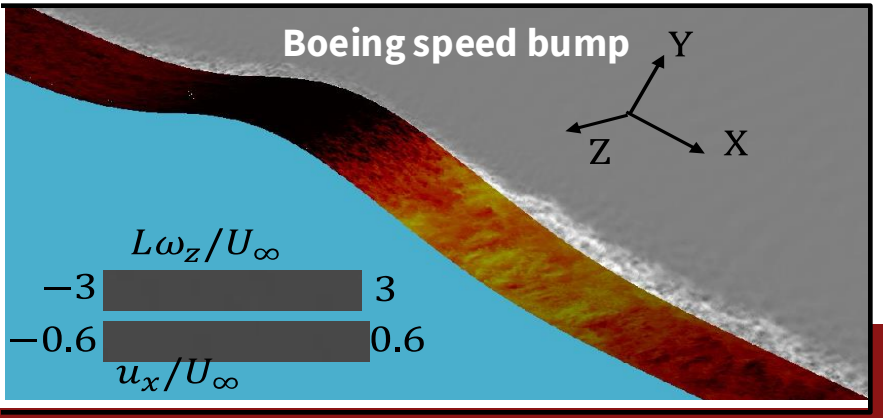


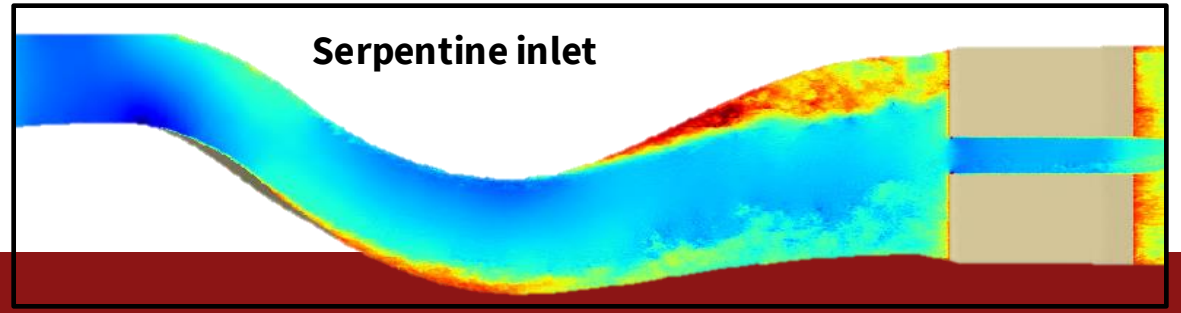












Questions?

CTR | Stanford University
CENTER FOR TURBULENCE RESEARCH